INTERNATIONAL ATOMIC ENERGY AGENCY
UNITED NATIONS EDUCATIONAL, SCIENTIFIC AND CULTURAL ORGANIZATION
INTERNATIONAL CENTRE FOR THEORETICAL PHYSICS
I.C.T.P., P.O. BOX 586, 34100 TRIESTE, ITALY, CABLE: CENTRATOM TRIESTE

H4.SMR/942-12

Third Workshop on 3D Modelling of Seismic Waves Generation Propagation and their Inversion

4 - 15 November 1996

Inverse Problems in Source Parameter Retrieval

J. Sileny
Geophysical Institute
Academy of Sciences
Cech Republic

Inverse problems in source parameter retrieval

Lecture notes to the Third Workshop on
"Three-Dimensional Modelling of Seismic Waves"
4-15 November 1996

Jan Šílený

GFÚ

Geophysical Institute
Acad. Sci. Czech Rep.
Boční II/1401
14131 Praha 4
Czech Republic

Tel +42-2-67103071
Fax +42-2-761549
E-mail jsi@ig.cas.cz
sileny@mbox.cesnet.cz

Introduction

The topic represents a vast pool of problems where several parallel hierarchies can be traced in dependence of the viewpoint of the ordering. Let's mention three of them which may be marked as the major ones: (i) ordering according to source model accepted, (ii) according to the type of information used to retrieve the source parameters within the model selected, (iii) ordering according to the frequency content of the input data which reflects combined effect of the magnitude and distance of the seismic event. The hierarchies (ii) and (iii) are not independent, of course: (iii) is a subspace of (ii), being another way of sorting the seismic information. We are keeping it here separately because the frequency content is a principal feature of seismic data according to which inverse methods are designed.

The most important viewpoint for sorting the inverse methods is complexity of the model accepted for description of the physical processes occuring in the earthquake focus. Two principal cathegories of the source models may be distinguished: kinematic models, where field of dislocations or equivalent forces is phenomenologically specified in the source region and care is not taken whether the particular distribution is able to be physically realized, and dynamic models which determine the dislocations on the basis of solving a physical problem of rupturing the stressed material or slipping along a pre-existing fault with specified friction characteristics. In general, the forward problem, i.e. determination of seismic wavefields supposing specified input assumptions, is much more difficult for dynamic models than for the kinematic ones. For example, forward problem for a Haskell-type fault includes determination of seismic displacement due to rupturing a rectangular area with fixed velocity of dislocation propagation. Forward problem for an analogous dynamical model means to construct the wavefield, too, but comprises much more effort, namely the search for the dynamics of the rupture itself: its spontaneous life within specified outer conditions as, e.g., the stress field and rheology of the medium. Due to high claims of the dynamic source models both to the parametrization of the model and to mathematical tools for handling it, no inverse solutions dealing with dynamic models are known to the author of this review.

On the other hand, plenty of inverse methods have been developed dealing with kinematic models which describe only phenomenologically physical processes occuring in earthquake foci. Within this cathegory we may mark two major approaches to tackle the focus: as a point if its real size is small comparing to the length of waves investigated, and considering its finite extent in the opposite case. In the following we constrain ourselves to inverse problems dealing with sources in point approximation, as finite-extent sources have been discussed elsewhere within this course.

At present, in the approaches to invert seismic data with the aim to determine point source characteristics the moment tensor description is almost exclusively used. Its advantage is, in principle, dual: first, on the contrary to former double-couple description it is more general, as it comprises besides the equivalent of shear dislocation also additional components describing other modes of fracturing, at the first hand the volumetric component. Second, it results in linear inverse problems that are computationally highly advantageous.

The idea to describe the source by moment tensor originates with the fact that tectonic earthquakes are seismic sources of internal origin, with action of no external forces and moments, where the force and moment equilibrium is preserved. This is just the characteristics of couples and double couples without moment which constitute the

moment tensor (see Fig.AR1 reprinted from Aki and Richards, 1982). A more rigorous and general method of representation was developed by Backus and Mulcahy (1976, 1977) who define a seismic source as a deviation from elastic deformation: the stress tensor is constituted from the elastic part and the inelastic one called stress glut. The latter one is expanded into a series of moments from which usually the lowest one is retained, which is just the seismic moment tensor, a symmetric tensor of 2nd order described by 6 components.

However, the moment tensor is not the most general description of a seismic source. Takei and Kumazawa (1995) pointed out that formulation by Backus and Mulcahy (1976) which introduced general moment source was not adequate to describe single force and torque events. In addition to the sress glut by Backus and Mulcahy which represents a departure from a linear stress-strain relationship in the source region, they introduced inertial glut and gravitational glut allowing them to consider a mass advection in the source region. From these novel gluts they derived three types of 'vector-type' equivalent force components which should complement the traditional tensor-type components: (1) a single force, produced by the motion of the gravitational centre of the source region relatively to the surrounding medium, (2) a torque, produced by the change of the angular momentum and the gravitational loading in the source region, and (3) a pressure dipole, produced by a change of the pressure gradient in the source region. This source model is significant especially when volcanic earthquakes are treated in the foci of which the flow of molten magma represents a momentum exchange with the surounding medium, that can be phenomenologically described as a single force. Another type of seismic sources for which the single force description is adopted are landslides. The Figs.TK1-2 (reprinted from Takei and Kumazawa (1995)) show physical models of the sources discussed and the P-displacements, respectively. Fig.TK3 demonstrate that radiation effectivity of the single-force focus is even higher than that of the DC source.

Paralelly we shall consider also another hierarchy of inverse methods, namely from the viewpoint of the information used as input data of the inverse problem. The extent and quality of the available information is the key factor which sets limits on the model of the source that can be determined in the inverse problem. The extent of seismic information ranges from first signs which, in fact, take a single bit only from the whole seismogram, through amplitudes or amplitude ratios, where the "yes-no" information of first signs is complemented with information "how much", to exploiting besides signs and amplitudes also the shape of individual wavegroups or of complete seismogram. Most of inverse methods inherently contain construction of the synthetic "data" for a generic model of the source which is in the course of inversion compared to observed data and according to their match the parameters of the source model are adjusted. Therefore, inclusion of the data of high information content within the above described sequence signs-amplitudes-waveforms simultaneously represents high claims concerning construction of synthetic data, i.e. in the forward modelling. Whereas to model the signs only, a rough estimate of the structure is sufficient as they do not depend on fine details of the structure, for modelling amplitudes much more expertise is needed because they are influenced not only by distribution of velocity but also the attenuation, and, finally, modelling the waveforms demands complete knowledge of the medium. Thus, the application of a particular method from the viewpoint of the hierarchy just discussed is conditioned not only by our skill in mastering sophisticated inverse schemes but also by the level of knowledge of the medium in the area under study which is available at the moment.

For completeness, when listing information content of data connected to various source models, let's mention again the dynamic source models. On the contrary to kinematic (phenomenological) models which exploit information contained in seismic records, the dynamic models need more: besides the rheological parameters which rule seismic velocities and their attenuation also the medium characteristics governing the rupturing the material like dislocation energy are in the game. That is, dynamic models require, in general, also a non-seismic information.

General formulation of inverse problem for seismic source

Limiting our consideration to kinematic source models in the definition presented above, generally the synthetic seismic characteristics which is in an inverse scheme compared to observed seismic data, depends both on the source and on the medium in which the signal generated in the source propagates towards the observer:

$$seismic\ wavefield\ =\ [\ source\ \otimes\ medium\ ]$$

The left-hand side may be represented by signs, amplitudes or waveforms. The "source" on the right-hand side is a term comprising goniometric functions of dip, strike and rake angles and the slip amplitude if the source is described by the double couple model, it is seismic moment tensor in the namesake formalism, or it may comprise vector-type components in the more general description by Takei and Kumazawa. The item "medium" summarizes the involvment of the medium in the seismic wavefield represented by the Green function - response of the medium to the elementary modes of the excitation. The symbol $\otimes$ represents the operation that relates the quantities describing the source and the medium: the convolution in the time domain and multiplication in the frequency domain. The brackets in the RHS generalize the summation of contributions of individual elementary source in the finite-extent focus - integration along a surface for sources represented by faults and integration over a volume in the case of more general types of foci. In particular, seismic displacement at the point of an observer $\mathbf{r}$ generated by a moment-type source distributed along a fault surface can be expressed in the form

$$u_k(\mathbf{r},t) = \iint_S \int_\tau M_{ij}(\xi,\tau)\, G_{ki,j}(\mathbf{r},\xi,t-\tau)\, d\tau\, dS, \qquad (1)$$

for a focus small comparing to wavelengths investigated it is reduced to

$$u_k(\mathbf{r},t) = \int_\tau M_{ij}(\xi,\tau)\, G_{ki,j}(\mathbf{r},\xi,t-\tau)\, d\tau, \qquad (2)$$

or, in the frequency domain, to

$$u_k(\mathbf{r},\omega) = M_{ij}(\xi,\omega)\, G_{ki,j}(\mathbf{r},\xi,\omega). \qquad (3)$$

The preceding equations illustrate the dual influence of the source and the medium in the seismic information. The inverse problem for seismic source in this representation means to determine the moment tensor M_{ij} from the wavefield u_k, thus, the effect of the medium introduced in the Green function G_{ki} must be eliminated from the seismograms.

The way of the annihilation of the medium effect constitutes additional sorting of inverse problems. Sometimes we are able to construct the Green functions directly. To do that we must be sure enough in the parameters of the medium in the area under study. The information on the medium must be as complete as possible, because in the opposite case the structural details which are not properly modelled in the Green function are projected in the source where they appear as spurious signals. Let's call the algorithms which search for the source description from (2) or (3) by using explicit modelling the Green function *absolute inverse methods*. However, in practice, the opposite case is frequent, namely that there is not enough information even to decide about the type of the model (mode of layering, dimensionality of the inhomogeneity, attenuation law, anisotropy, etc.), and if the type can be chosen then rarely there is sufficient data to fix the values of its parameters. Then, to proceed in the task of the source retrieval, algorithms have been developed which simply utilize records of weak events as the Green function or take advantage of group processing of tightly clustered events. Although the principles of avoiding the disability to model directly the Green function in both the approaches are different, let's summarize them in the cathegory named *relative methods*.

In the following chapters we shall describe in more detail some of the methods listed above. We shall follow the ordering of inverse problems from the viewpoint of the extent of seismic information exploited from the records combined with the way in which the source is parametrized, and demonstrate these methods by brief browsing through the papers in which either they were introduced, or extended in an interesting way or well described from the viewpoint of the tuition. The list will far be not complete and will be very subjective converging naturally to the approaches in which the author of this review has a personal experience. Moreover, some methods range more cathegories (e.g., linear programming algorithm may process simultaneously both the signs and amplitudes), thus, the ordering is not unambiguous.

I. Absolute methods

As defined in the preceding chapter, as absolute methods we shall understand those approaches which use explicit modelling the Green function when solving (2) or (3).

Double couple description

Double couple is the force equivalent of a pure shear dislocation - a tangential slip along a planar fault. If we omit the determination of its strength, double couple is defined by 3 parameters, usually the dip, strike and rake (slip) angles (dip and strike determine the orientation of one of the two nodal planes, the rake defines the slip direction which is the normal of the other nodal plane (see Fig.P1, reprinted from Pearce, 1977). The advantage of small number of parameters to be determined is degraded by nonlinear dependence of seismic wavefield, which demands robust search algorithms.

Double couple is the source model which is exclusively accepted when analysis of only signs of seismic phases is performed. We skip these methods because they are rarely applied at present and if they are, the motivation is to process seismic data from pre-digital epoch. In the following we mention shortly methods that use amplitude

ratios as input data. The principle advantage of the methods using amplitude ratios is the fact that the ratio should be less sensitive to the details of the structure than the amplitudes themselves. The ratio of z-component of SV and P waves was inverted by Kisslinger et al. (1981). They used a grid-search algorithm for strike and dip with a priori selected value of rake specified on the basis of, e.g., geological or tectonic information. With the aim to determine the DC orientation for shallow earthquakes, Pearce (1977) developed the algorithm to invert relative amplitudes of P and pP waves. This approach benefits from the fact that thanks to the similarity in their paths, P and pP waves suffer the same fractional loss of amplitude during their propagation except near the source (Fig.P2, reprinted from Pearce, 1977). Pearce defined the acceptable range of P and pP amplitude ratio and performed a systematic search for all source orientations which are compatible with acceptable intervals of the ratios. He displayed the orientations in a grid in the dip-rake plane where strikes were visualized by rotating a pointer-arrow, see Fig.P3. As it is common for grid-search algorithms, the model space is regularly explored and the region (or regions) of acceptable solutions are mapped, which enables us to make a guess of the uniqueness and confidence of the solution. Pearce demonstrated his method by processing the data from the Kazakhstan 1969 earthquake (Fig.P4) which yielded a well confined region of acceptable orientations of the DC (Fig.P5).

Moment tensor description

Moment tensor as a quantity which depends both on source strength and its orientation was introduced in seismology by Gilbert (1971), who also suggested that, since the waveforms are linear functionals of its six independent components, this property could be advantageously utilized in formulating the inverse problem for the source mechanism. Apart from the context of normal modes excitation which was considered by Gilbert, moment tensor formalism was applied to modelling the generation of both surface and body waves. In the former cathegory the papers by, e.g., Mendiguren (1977) and Aki and Patton (1978) can be mentioned. As to to latter one, the paper by Ward (1980) was the first practical application of the moment tensor approach to the retrieval of the mechanism from the waveforms of body waves. Thanks to shorter wavelength, body waves have a greater resolving power than surface waves, however, on the other hand, to model them properly we need to know much finer details of the structure, which is commonly a big problem.

Joint inversion of signs, amplitudes and amplitude ratios

It was already noted in the preceding chapter that in the inhomogeneous medium the amplitudes of seismic waves are considerably distorted while suitably chosen ratios of amplitudes are affected much less. The trick is to choose seismic phases that follow similar paths, such as P/SV, P/SH or SV/SH. If the ratio of velocities of the waves involved is constant, which usually is a good approximation, then the ratio of the amplitudes is unaffected by the propagation. This is a great advantage because it is common that our information on the complexities of the medium is not detailed enough to allow us to reconstruct the amplitudes on the focal sphere successfully. However, there is also a drawback at the same time: amplitude ratios are severely nonlinear and require computationally intensive searching methods.

Julian and Foulger (1996) suggested the trick how to invert amplitude ratios within the scheme of linear programming and, thus, to process them in a unified method together with signs and amplitudes (following the preceding algorithm by Julian, 1986).

Linear programming is, by definition (Press et al., 1992), the algorithm which for N independent variables $x_1,\ldots,x_N$ maximizes the function ("objective function")

$$z = a_{01}x_1 + a_{02}x_2 + \ldots + a_{0N}x_N$$

subject to primary constraints of non-negativity of x_k, and to $M=m_1+m_2+m_3$ additional constraints:

$$\begin{aligned} a_{i1}x_1 + \ldots + a_{iN}x_N &\le b_i \ge 0 \qquad & i &= 1, \ldots, m_1 \\ a_{j1}x_1 + \ldots + a_{jN}x_N &\ge b_j \ge 0 \qquad & j &= m_1 + 1, \ldots, m_1 + m_2 \\ a_{k1}x_1 + \ldots + a_{kN}x_N &= b_k \ge 0 \qquad & k &= m_1 + m_2 + 1, \ldots, m_1 + m_2 + m_3 \end{aligned}$$

There is no limit to the number of constraints M with respect to N. A vector $(x_1,\ldots,x_N)$ satisfying all the constraints is called a feasible vector, that one which maximizes the objective function is called the optimal feasible vector. In the N dimensional space, the linear constraints are hyperplanes and by imposing each constraint a part of the space is selected as a possible locus of feasible vectors. Applying all the constraints, the feasible region is all bounded by hyperplanes - geometrically it is a convex polyhedron ("simplex"). Since the objective function is linear, it cannot have maximum inside but somewhere on the boundary. The linear optimization algorithm just follows individual "ribs" of the simplex in the direction where the objective function is increased. According to Julian and Foulger (1996), modelling the signs, amplitudes and amplitude ratios can be described in inequalities. Expressing the amplitude of a seismic wave as $\mathbf{u} = \mathbf{g}^T\mathbf{m}$ where $\mathbf{g}$ is a column six-vector of Green functions for the particular wave and $\mathbf{m}$ the vector from moment tensor components, a polarity observation is expressed as

$$\mathbf{g}^T\mathbf{m} \le 0 \quad \text{or} \quad \mathbf{g}^T\mathbf{m} \ge 0,$$

and amplitude observation described as a pair of inequalities

$$\mathbf{g}^T\mathbf{m} \le a_{max} \quad \text{and} \quad \mathbf{g}^T\mathbf{m} \ge a_{min}$$

where a_{min} and a_{max} are lower and upper bounds on the particular amplitude observation. Amplitude ratios may be treated similarly:

$$\frac{u^{(1)}}{u^{(2)}} \le r_{max}, \quad \frac{u^{(1)}}{u^{(2)}} \ge r_{min}$$

that is

$$\mathbf{g}^{(1)T}\mathbf{m} \le r_{max}\,\mathbf{g}^{(2)T}\mathbf{m}, \quad \mathbf{g}^{(1)T}\mathbf{m} \ge r_{min}\,\mathbf{g}^{(2)T}\mathbf{m}$$

$$(\mathbf{g}^{(1)T} - r_{max}\,\mathbf{g}^{(2)T})\,\mathbf{m} \le 0, \quad (\mathbf{g}^{(1)T} - r_{min}\,\mathbf{g}^{(2)T})\,\mathbf{m} \ge 0.$$

These inequalities are of the same form as those for the polarity observation but with different Green function.

The objective function to be minimized is the L_1 norm of the residuals

$$F = \sum_{i \in P} |u_i| + \sum_{i \in Q} |u_i - a_i| + \sum_{i \in R} \left| u_i^{(1)} - r_i u_i^{(2)} \right|,$$

where P is the set of polarity constraints that are not satisfied, and Q and R is the set of unsatisfied amplitude and amplitude-ratio constraints, respectively. On the observation of an earthquake from a volcanic area in Iceland, Julian and Foulger demonstrated the disability of the signs only to resolve the type of the mechanism (explosive, implosive or double couple), see Fig. JF1. On the contrary, amplitude ratios posses the capacity to decide which type is more appropriate: see Fig. JF2, where the fit of the amplitude ratios is much better for the best-fitting general moment tensor source (with a non-zero volumetric component) then in the case that a double couple is prescribed. Fig. JF3 explains construction of the arrow representing the ratio of amplitudes A and B. Fig. JF4 informs us on the polarities of the best-fitting source model. Besides signal amplitudes and ratios, Julian and Foulger designed a formalism to process unsigned amplitudes and absolute amplitude ratios as well.

Moment tensor from waveforms

Stump and Johnson (1977) took advantage of the linear relation between seismic amplitude and the moment tensor and designed a linear scheme to invert records of body waves. In both the time and frequency domain it can be written in the matrix form

$$\mathbf{u} = \mathbf{G}\,\mathbf{m}$$

Time domain: **u** : sampled values of ground displacement stacked for components and stations; dimension n

G : n x 6 matrix of Green functions

m : vector of 6 components of the moment tensor (temporal dependence; i.e., the source time function is supposed to be known a priori)

Frequency domain: **u** : complex values → dimension 2n

G : dimension 2n x 12

m : dimension 12

In the frequency domain, thanks to the fact that each frequency is considered separately, the temporal dependence of the moment tensor is determined, too. Depending on the value of n the problem is underdetermined (n<6), exact (n=6) or overdetermined (n>6).

Stump and Johnson proposed to use singular value decomposition of **G**:

$$\mathbf{G} = \mathbf{W}\mathbf{Q}\mathbf{V}^{\mathrm{T}},$$

where **W** consists of eigenvectors associated with nonzero eigenvalues of $\mathbf{G}\mathbf{G}^{\mathrm{T}}$, **V** is constructed similarly but from $\mathbf{G}^{\mathrm{T}}\mathbf{G}$, and on the diagonal of **Q** there are positive roots of p nonzero eigenvalues of $\mathbf{G}^{\mathrm{T}}\mathbf{G}$. The generalised inverse of **G** becomes

$$\mathbf{G}^{-1} = \mathbf{V}\,\mathbf{Q}^{-1}\,\mathbf{W}^{\mathrm{T}}$$

According to the magnitude of the eigenvalues, it informs us which parameters are resolved well and vice versa. In the case the eigenvalue associated with a particular

parameter equals zero, the generalized inverse provides us with no information on this parameter.

Teleseismic waveforms

If we speak of mechanisms in the moment tensor formalism, determined by inverting seismic waveforms from teleseismic distances, we usually understand Harvard solutions. It is the method by Dziewonski, Chou and Woodhouse (1981) which uses normal-mode approach to the modelling of the Green function and an iterative scheme to determine the moment tensor components and, simultaneously, the centroid location - location of the "best" point source. Normal mode approach synthetizes wavefields of very long wavelenghts and in the case all the modes are included the synthesis is exact: all theoretically predictable seismic arrivals (surface waves as well as body waves) are automatically included. For the source description the moment tensor formalism is applied. The seismic wavefield is composed of the contributions of moment tensors of various degrees which originate from the expansion of the stress glut of Backus and Mulcahy. Apart from the zero-th term $M_{ij}^{(0,0)}$ the subsequent terms explicitly include space-time coordinates $(\mathbf{r}_s,t_s)$ of the point around which the expansion was performed

$$M_{ij}^{(0,0)} = \int_t \int_V \Gamma_{ij}(\mathbf{r},t)\, dV\, dt$$
$$M_{ijp}^{(1,0)} = \int_t \int_V \Gamma_{ij}(\mathbf{r},t)\, (r_p - r_{sp})\, dV\, dt$$
$$M_{ijpq}^{(2,0)} = \int_t \int_V \Gamma_{ij}(\mathbf{r},t)\, (r_p - r_{sp})(r_q - r_{sq})\, dV\, dt$$
$$M_{ij}^{(0,1)} = \int_t \int_V \Gamma_{ij}(\mathbf{r},t)\, (t - t_s)\, dV\, dt$$
$$M_{ij}^{(0,2)} = \int_t \int_V \Gamma_{ij}(\mathbf{r},t)\, (t - t_s)^2\, dV\, dt$$
$$\vdots$$

Because of the freedom in specifying the point $(\mathbf{r}_s,t_s)$, the higher moments are not intrinsic properties of the source To obtain them independent of the arbitrary locus, a special point is selected which represents in some sense the "centre" of the distribution of the stress glut in space and time. For a scalar field the centroid would be the convenient point, which is defined (1) either as the point about which the 1st moments vanish or (2) the point about which the 2nd moments are individually minimized. However, for a tensor field like stress glut there is, in general, no point satisfying either (1) or (2). Therefore, Backus defined the centroid for the stress glut as the point about which the sum of squares of the 1st moments is minimum. Then, this point represents the "best" location for an equivalent point source both in space and time.

First moments in the centroid $(\mathbf{r}_c,t_c)$ and in the reference point $(\mathbf{r}_s,t_s)$ are related by

$$M_{ijp}^{(1,0)}(\mathbf{r}_c) = (r_{sp} - r_{cp})\, M_{ij}^{(0,0)} + M_{ijp}^{(1,0)}(\mathbf{r}_s)$$
$$M_{ij}^{(0,1)}(t_c) = (t_s - t_c)\, M_{ij}^{(0,0)} + M_{ij}^{(0,1)}(t_s)$$

which introduces the centroid location in the term for the modal excitation (synthetic wavefield) and enables us to invert for it. Dziewonski, Chou and Woodhouse (1981) designed the inverse scheme for simultaneous retrieval of zero-order moment tensor $M_{ij}^{(0,0)}$ and the displacement of the centroid from a reference point $(\Delta\mathbf{r},\Delta t)=(\mathbf{r}_c-\mathbf{r}_s,t_c-t_s)$. They represented seismic wavefield as

$$u_i(\mathbf{r},t) = \Sigma_{j=1,\ldots,6}\, f_j\, \phi_{ij}(t) + \mathbf{b}_i(t,f_j)\, \Delta\mathbf{r} + c_i(t,f_j)\, \Delta t,$$

where in f_k the components $M_{ij}^{(0,0)}$ are stored. The excitation functions ϕ_{ij} are independent of f_k, thus the 1st term leads to a linear estimation procedure for f_k. The functions $\mathbf{b}_i$ and c_i depend also of the moment tensor components f_k, which requires an iterative procedure to refine the location of the centroid. The inversion method has been automated and for more than a decade has been used for routine determination of mechanisms of moderate earthquakes around the globe. Up to now more than 10000 solutions were obtained, which contributed much to our knowledge on the seismicity and stress state in active zones.

A powerful method for the recovery of a time-dependent moment tensor source from waveform data was designed by Sipkin (1982). It is based on multichannel signal-enhancement theory: the Green functions are considered to be the multichannel input, the moment rate tensor is viewed as the convolution filter operating on the input, and the observed seismograms are the desired output. Using recursion techniques, the elements of the moment rate tensor are solved for as the optimum multichannel signal-enhancement filter. The method considers each element of the moment rate tensor as an independent function of time. However, it is within the capacity of the method to avoid searching for the time dependence of the moment rate tensor simply by limiting the filter to a length of one.
If we concatenate the N seismograms to be inverted into the vector $\mathbf{u}$ and the corresponding Green functions to the 6 vectors $\mathbf{g}_k$, the convolution

$$\mathbf{u}(t) = \Sigma_{k=1\ldots6}\, \mathbf{m}_k(t) \otimes \mathbf{g}_k(t)$$

may be written in matrix form

$$\begin{bmatrix} u(0) \\ u(t_1) \\ u(t_2) \\ \vdots \\ \vdots \\ \vdots \\ \vdots \\ \vdots \end{bmatrix} = \begin{bmatrix} g_1(0) & g_2(0) & \ldots & g_6(0) & 0 & \ldots & & & 0 \\ g_1(t_1) & g_2(t_1) & \ldots & g_6(t_1) & g_1(0) & g_2(0) & \ldots & g_6(0) & 0\ldots0 \\ g_1(t_2) & g_2(t_2) & \ldots & g_6(t_2) & g_1(t_1) & g_2(t_1) & \ldots & g_6(t_1) & g_1(0)\ldots \\ \vdots & \vdots & & \vdots & g_1(t_2) & g_2(t_2) & \ldots & g_6(t_2) & g_1(t_1)\ldots \\ \vdots & \vdots & & \vdots & \vdots & \vdots & & \vdots & g_1(t_2)\ldots \\ \vdots & \vdots & & \vdots & \vdots & \vdots & & \vdots & \vdots \\ \vdots & \vdots & & \vdots & \vdots & \vdots & & \vdots & \vdots \\ \vdots & \vdots & & \vdots & \vdots & \vdots & & \vdots & \vdots \end{bmatrix} \begin{bmatrix} m_1(0) \\ m_2(0) \\ \vdots \\ m_6(0) \\ m_1(t_1) \\ \vdots \\ m_6(t_1) \\ \vdots \end{bmatrix}$$

or, $\mathbf{u} = \mathbf{G}\,\mathbf{m}$.

If we introduce the autocorrelation and crosscorelation operators

$$a_{ij}(s) = \Sigma_t\, g_i(t)\, g_j(t+s), \qquad c_i(s) = \Sigma_t\, g_i(t)\, u(t+s),$$

then the terms appearing in the normal equations $\mathbf{m} = (\mathbf{G}^T\mathbf{G})^{-1}\mathbf{G}^T\mathbf{u}$ take the form

$$\mathbf{G}^T\mathbf{u} = [c_1(0),\ldots, c_6(0), c_1(t_1),\ldots, c_6(t_1),\ldots] = \mathbf{c},$$

$$\mathbf{G}^T\mathbf{G} = \mathbf{A} = \begin{bmatrix} a_{11}(0) & \ldots & a_{16}(0) & a_{11}(-1) & \ldots & a_{16}(-1) & a_{11}(-2) & \ldots & a_{16}(-2) & \ldots \\ \vdots & & \vdots & \vdots & & \vdots & \vdots & & \vdots & \\ a_{61}(0) & \ldots & a_{66}(0) & a_{61}(-1) & \ldots & a_{66}(-1) & a_{61}(-2) & \ldots & a_{66}(-2) & \ldots \\ a_{11}(1) & \ldots & a_{16}(1) & a_{11}(0) & \ldots & a_{16}(0) & a_{11}(-1) & \ldots & a_{16}(-1) & \ldots \\ \vdots & & \vdots & \vdots & & \vdots & \vdots & & \vdots & \end{bmatrix}$$

$$\begin{bmatrix} & & & & & & & & \\ a_{61}(1) & \dots & a_{66}(1) & a_{61}(0) & \dots & a_{66}(0) & a_{61}(-1) & \dots & a_{66}(-1) & \dots \\ a_{11}(2) & \dots & a_{16}(2) & a_{11}(1) & \dots & a_{16}(1) & a_{11}(0) & \dots & a_{16}(0) & \dots \\ \vdots & & \vdots & \vdots & & \vdots & \vdots & & \vdots & \\ a_{61}(2) & \dots & a_{66}(2) & a_{61}(1) & \dots & a_{66}(1) & a_{61}(0) & \dots & a_{66}(0) & \dots \\ \vdots & & \vdots & \vdots & & \vdots & \vdots & & \vdots & \\ \vdots & & \vdots & \vdots & & \vdots & \vdots & & \vdots & \end{bmatrix}$$

After defining the submatrix blocks

$$\tilde{\mathbf{A}}(\tau) = \begin{bmatrix} a_{11}(\tau) & \dots & a_{16}(\tau) \\ \vdots & & \vdots \\ a_{61}(\tau) & \dots & a_{66}(\tau) \end{bmatrix} = \tilde{\mathbf{A}}^{T}(-\tau)$$

we can write the normal equation matrix

$$\mathbf{A} = \begin{bmatrix} \tilde{\mathbf{A}}(0) & \tilde{\mathbf{A}}(-1) & \tilde{\mathbf{A}}(-2) & \dots \\ \tilde{\mathbf{A}}(1) & \tilde{\mathbf{A}}(0) & \tilde{\mathbf{A}}(-1) & \dots \\ \tilde{\mathbf{A}}(2) & \tilde{\mathbf{A}}(1) & \tilde{\mathbf{A}}(0) & \dots \\ \vdots & \vdots & \vdots & \end{bmatrix}$$

The matrix **A** has a special symmetry (block-Toeplitz form) that can be solved by using recursive techniques, which offer savings in both the time and storage. Thanks to the advantages of this formulation even large matrices can be treated, i.e. long time series in the moment rate tensor may be considered.

Local waveforms

Sipkin (1982) demonstrated the method on teleseismic data. Application to local waveforms needs several extensions of the algorithm. First, local seismograms contain high frequencies, which results in numerical problems when solving the normal equations. Koch (1991) pointed out this effect and proposed to introduce the damping

$$\mathbf{m} = (\mathbf{G}^{T}\mathbf{G} + \theta^{2}\mathbf{I})^{-1}\mathbf{G}^{T}\mathbf{u} \qquad (1)$$

When treating local data, more accurate model of the medium is needed than a smoothed one suited in low frequencies. Our ignorance about the model results in erroneous Green function which further may be made even worse due to imprecise location of the event. An attempt to address this problem was made by Šílený et al. (1992) and Šílený and Pšenčík (1995), who extended the Sipkin's method by introducing an iterative loop in which hypocentra in an a priori selected region are tested and also a simplistic variation of the structural model is introduced.

The method consists of two closely related parts which we will refer to as (I) and (II). In the first one, the linear inversion is used to invert the observed data for a specified hypocentral point and for a specified structural model. This part provides the mechanism of the source. On the basis of the retrieved mechanism the synthetic seismograms are constructed and compared with the observed records. The L_2-norm of their difference is a measure of a 'success' of the inversion in this point. The value of the residual norm is of a principal significance in the second part of the method. It is an inversion scheme, in which the hypocentral coordinates and the structural weighting factor are being determined in an iterative procedure with the criterion of minimization

of the residual norm of synthetics and data. It means that the linear step providing the mechanism is an 'elementary cell' of the method, which is multiply performed in the iterative scheme updating the hypocentral coordinates and structural weighting factor(s).

I. In the linear step the Sipkin's inversion with damping is performed. Its output is a set of six moment tensor rate functions (MTRFs) that are generally independent, which implies time dependent mechanism. Since for weak events we do not anticipate a change in the mechanism during the rupture process, we try to factorize the MTRFs to exclude a time variation from them. The MTRFs can be tested for linear dependence by looking for common source time function $\dot{m}(t)$ and six multiplicative constants M_{ij} (i=1,...3; j=i,...,3) which minimize the normalized L_2 norm of the residuals

$$N_r = \left\{ \sum_{i=1}^{3} \sum_{j=i}^{3} \int_0^T \left[\dot{M}_{ij}(t) - M_{ij} \dot{m}(t) \right]^2 dt \right\}^{\frac{1}{2}} \times \left\{ \sum_{i=1}^{3} \sum_{j=i}^{3} \int_0^T \left[\dot{M}_{ij}(t) \right]^2 dt \right\}^{-\frac{1}{2}}$$

Here T is the duration of the whole rupture process. If the minimization of N_r with respect to $\dot{m}(t)$ and M_{ij} quantities is successful, i.e. if $N_M << 1$, we arrive to constant mechanism of the event described by the moment tensor M_{ij} and time dependence of the rupture given by $\dot{m}(t)$.

Factorization of the MTRFs was addressed as a function minimization problem: the residual sum N_r was treated as a non-linear function of N_t+6 parameters (N_t is the number of triangles used for parameterization of the MTRFs) by using the Monte Carlo and simplex minimization schemes. An alternative approach is a genetic algorithm which offers, besides its inherent robustness, an advantageous way to estimate simultaneously the uniqueness and confidence of the solution.

The problem of factorization of the MTRFs was also investigated by Ruff and Tichelaar (1990) and Vasco (1989). The former authors determine the source time function as a weighted average of the MTRFs, which needs some a priori idea about the mechanism to sum individual MTRFs with proper signs. The procedure of Vasco is based on singular value decomposition of the MTRFs into 'principal components'. The part corresponding to the biggest singular value is declared to be the best source time function and significance of the other components is checked by the F test. This approach is very effective and computationally straightforward, but it may happen that the individual principal components do not reflect real physical mechanisms in case they are not well separated in time.

II. On the basis of the MTRFs evaluated in a generic point during the step (I), the synthetic seismograms can be constructed and compared with observed records. We introduce the L_2 norm of their difference

$$N_s = \left\{ \sum_{k=1}^{N} \sum_{i=1}^{3} \int_0^T \left[u_i^k(t)|^{obs} - u_i^k(t) \right]^2 dt \right\}^{\frac{1}{2}}$$

as a measure of success of the linear inversion. Here N is number of 3-component stations yielding the data, $u_i^k(t)|^{obs}$ is the i-th component of observed seismogram recorded by the k-th station, $u_i^k(t)$ is the corresponding synthetic seismogram. To include the variation of hypocentral point and structural model into the method we

consider the Green functions $g_{ki,j}$ to be dependent on additional parameters q_l, l=1,...,M, which results in dependence of the norm N_S on the q_l parameters as well,

$$N_S = N_S(q_l)$$

The optimization of hypocentre localization and of structural model consists in minimization of the norm N_S with respect to the q_l parameters.

The parameters q_l comprise the following quantities:

1. Hypocentre coordinates: $q_1=z_H$, $q_2=x_H$, $q_3=y_H$

2. Weighting factor(s) describing interpolation between two models of the medium. There are two options:

a) The same structural model determined by interpolation is related to all the stations. Then we introduce a parameter q_4 ($0 \le q_4 \le 1$), where $q_4=0$ implies the Green functions computed for a model A, while $q_4=1$ indicates Green functions for a model B (the construction of Green functions for $0<q_4<1$ from $g_{ki,j}^A$ and $g_{ki,j}^B$ is described later). Here M=4.

b) Structural interpolation is performed for each station separately. In this case the number of weighting factors for structural interpolation is the same as the number of stations. Specifically, we have N parameters $0 \le q_{j+3} \le 1$, j=1,...,N. A particular parameter q_{j+3} controls evaluation of Green functions for the j-th station in a similar way as in a): $q_{j+3}=0$ and $q_{j+3}=1$ imply selecting $g_{ki,l}^A$ and $g_{ki,l}^B$ for the j-th station, respectively. In this case M=N+3.

The requested minimization of the norm $N_S(q_l)$ can be performed either by a linearization approach or by a point-by-point evaluation of the function (5) in a grid-search for its minimum

The method proved to be effective in synthetic tests simulating configuration of a local network in Slovakia. The two alternative models of the medium (Fig.SP1: depth dependence of the velocities only; and SP2: 3-D inhomogeneity) yield a considerable shift in station projections onto the focal sphere (Fig.SP3). Direct P and S were generated for the strike-slip and dip-slip mechanisms with a simple Müller pulse time function (Fig.SP4). The relocation was successful in the horizontal coordinates but not in the depth, structural parameter was resolved properly, see Fig.SP5. The source time function was determined perfectly, as to the mechanism the result was better with the strike slip, see Figs.SP6 and SP7.

Error analysis: For an estimate of errors imposed on the moment tensor rate functions by presence of random noise in the input seismograms the general theory of inverse problems developed by Tarantola (1987) was applied. He showed that for Gaussian shape of a priori data probability and probability of forward modelling and in the case of linear forward problem $\mathbf{g(m)=Gm}$ the a posteriori marginal density $\sigma_M(\mathbf{m})$ is Gaussian, too:

$$\sigma_M(\mathbf{m}) \sim \exp[-\tfrac{1}{2}(\mathbf{m}-\langle\mathbf{m}\rangle)^T \mathbf{C}_M^{-1}(\mathbf{m}-\langle\mathbf{m}\rangle)], \qquad (2)$$

where

$$\langle\mathbf{m}\rangle = (\mathbf{G}^T\mathbf{C}_D^{-1}\mathbf{G} + \mathbf{C}_M^{-1})^{-1}\,(\mathbf{G}^T\mathbf{C}_D^{-1}\mathbf{d}_0 + \mathbf{C}_M^{-1}\mathbf{m}_0) \qquad (3)$$

$$\mathbf{C}_{M'} = (\mathbf{G}^T\mathbf{C}_D^{-1}\mathbf{G} + \mathbf{C}_M^{-1})^{-1} \quad . \qquad (4)$$

Here $\mathbf{m}$ is the vector of model parameters, $\mathbf{m}_0$ a priori information on the model, $\mathbf{G}$ forward modelling operator, $\mathbf{C}_D=\mathbf{C}_d+\mathbf{C}_T$, $\mathbf{C}_d$ is the data covariance, $\mathbf{C}_T$ covariance of the forward modelling and $\mathbf{C}_M$ covariance of a priori model information. Eq.(3) specifies the maximum likelihood vector of model parameters and (4) its a posteriori covariance matrix.

Applying this approach to our problem, the a priori data uncerntainty is originated by noise superimposed on the seismic records, while the modelization uncerntainty is caused by the use of improper Green functions for the construction of synthetic seismograms, due to mislocation of the hypocentre and/or imperfect knowledge of the structural model. The core of the inversion step is eq.(1) which coincides, in fact, with (3) provided that a priori model information $\mathbf{m}_0 = \mathbf{0}$, and the damping constant corresponds to its inverse variance multiplied by the data variance: $\upsilon^2 = \sigma_d^2/\sigma_{M_0}^2$. It should be pointed out that to compare (1) and (3) we have to set $\mathbf{C}_d = \sigma_d^2\mathbf{I}$, $\mathbf{C}_M = \sigma_{M_0}^2\mathbf{I}$, i.e. all the data items must have the same variance σ_d and similarly the distribution of all the a priori estimates of the model parameters must be described by the same value of σ_{M_0}.

Eq.(4) provides us with a posteriori variances of the MTRFs which are used in the factorization step (II) for an estimate of the covariance matrix of the moment tensor M_{ij} and of the error bars of the source time function $\dot{m}(t)$. Having the variances $\sigma_{ij}(t)$ of the MTRFs at hand, we can replace the normalized residual sum N_r by the weighted residual sum

$$N_f = \sum_{i=1}^{3}\sum_{j=1}^{3}\int_0^T \frac{1}{\sigma_{ij}^2(t)}\left[\dot{M}_{ij}(t) - M_{ij}\dot{m}(t)\right]^2 dt \qquad (5)$$

In turn, N_f may be considered as a χ^2 function of 6 degrees and 1 degree of freedom and by observing its increase in the vicinity of the resultant M_{ij} and $\dot{m}(t)$, respectively, to map the confidence regions in an a priori selected probability level. Then, following Riedesel and Jordan (1989), by using first perturbation theory we can transform the covariance matrix of M_{ij} into confidence regions for its eigenvalues and eigenvectors (Šílený et al., 1996).

During numerical tests of the influence of a noise contamination on the resolution of the mechanism and the STF (for the station distribution and structural models used see Fig.SCP1) considerable dependence of the mechanism appeared even for noise-free data on the quality of the focal sphere coverage, see Fig.SCP2. A large spurious component was detected in the mechanism when only z-components of the ground motion were used, the effect was almost negligible with 3-component data. Experiment with noisy data when the contamination was gradually increasing confirmed larger error in determination of the volumetric (V) part of the source: the error bars of the STF for the V subevent from the double source (DC subevent followed by a V subevent) are larger than for the DC peak, see Fig.SCP3.

II. Relative methods

On the contrary to the absolute methods which we defined as inverse algorithms that use explicit Green function constructed for a model of the medium

between the earthquake focus and the station, as relative methods we shall understand those approaches which use waveforms of weak events as empirical Green function (EGF) or in which the Green function does not explicitly appear at all.

Most of the papers dealing with EGF are based on the contribution by Hartzell (1978) who used records of weak events as EGF to model a strong earthquake which occured within the region of hypocentra of the weak event. This approach is built on the assumption that the source time function of a weak event is a simple pulse. However, even if this were completely true, the problem is that the records comprise the information on the mechanism, too. Thus, this approach can yield only the source time function of the strong event.

Plicka (1995) extends this approach by considering the radiation pattern of the weak events used as the generators of the EGF. He supposes to have at a station records of n weak earthquakes for which the mechanisms are known. Then, from the linear relation between the seismogram and the moment tensor in the frequency domain

$u_i(\omega) = \Sigma_k M_k(\omega) G_{ik}(\omega)$ $\quad k=1,...,6$ (or 5 with the deviatoric constraint)

i ranges components and/or stations,

the system of n equations follows

$$\begin{bmatrix} u_i^1 \\ u_i^2 \\ \vdots \\ \vdots \\ u_i^n \end{bmatrix} = \begin{bmatrix} M_1^1 & M_2^1 & \dots & M_6^1 \\ M_1^2 & M_2^2 & \dots & M_6^2 \\ \vdots & \vdots & & \vdots \\ \vdots & \vdots & & \vdots \\ M_1^n & M_2^n & & M_6^n \end{bmatrix} * \begin{bmatrix} G_i^1 \\ G_i^2 \\ \vdots \\ G_i^6 \end{bmatrix}$$

$$\mathbf{u} = \mathbf{M}\,\mathbf{g}$$

where **u** and **M** are arrays of known parameters and **g** has to be determined. In the frequency domain the matrices are complex. For $n>6$ the system is overdetermined and, then, can be solved by least-square method which yields normal equations

$$\mathbf{M}^T\mathbf{u} = \mathbf{M}^T\mathbf{M}\,\mathbf{g}.$$

In the domain of complex numbers the $\mathbf{M}^T$ is complex conjugate to **M**. The solution is a set of 6 complex values of the spectrum of the Green function for the considered component/station. By repeating the procedure for more frequencies ω we can complete its spectrum and, finally, determine the Green function in the time domain.

Plicka tested the algorithm with synthetic records constructed by the discrete wavenumber synthesis. Since the EGF determination means schematically a division in the frequency domain

$$G(\omega) = u(\omega) \,/\, M(\omega),$$

it is very important to check the spectral bandwith of u and M. It is evident that when the bandwith of $M(\omega)$ is greater than that of $u(\omega)$, no problems appear and the bandwith of $G(\omega)$ is controlled by the bandwith of $u(\omega)$. However, in the opposite case for some frequencies the ratio $u(\omega)/M(\omega)$ may diverge, which originates spurious oscillations in the time domain of the EGF. This is illustrated in Fig.PL1 (convenient

relation of the spoectra of *u* and *M*, see parts B and D) and Fig.PL2 (inconvenient relation, see spurious signal in the EGF in E).

Ideally, all the *n* earthquakes with known mechanisms should have the same hypocentrum. In reality, of course, this is not the case: they are situated within a zone of a finite size. Then, the results are better the smaller is this zone. The scale is related to the wavelength of the records used: increasing the wavelength the EGF determination is more precise. Plicka demonstrated this by performing the inversion for high and low-frequency synthetic records, see Fig.PL3 and PL4, respectively. In the former case the ratio of the wavelength and the focal zone size is 1.5 for P and 0.8 for S waves, while in the latter one it reaches about 5 and 3 for P and S, respectively. By comparing Figs.PL3 and PL4 we can see that the reconstruction of the data by means of the resolved EGF is much better in the low frequencies (original data - thick line, reconstructed data - thin line).

Finally, Plicka applied the method to real data from the 1985 earthquake swarm in Western Bohemia, Czech Rep. (Fig.PL5, reprinted from Kolář, 1994). An example of the velocity record and its spectrum can be seen in Fig.PL6. The application of the algorithm to determine the EGF was very successful, as it can be seen from the good fit of the reconstructed signals (thin lines) with the observed records (thick lines) in Fig.PL7.

Apart from the relative methods that operate explicitly with the Green function, there is a group of algorithms which eliminate the Green function completely from the task of the mechanism retrieval. Some of them need to have an a priori knowledge of the mechanism ("reference mechanism"): the method by Patton (1980) designed for inversion of surface waves constructs it by considering two close earthquakes with different mechanisms. The difference of observed and calculated spectral ratios and residual differential phase are minimized with respect to depth of the events and their mechanisms. Then another event is added and the source parameters are revised. When after addition of a new event and revision of the pooled events their mechanisms are only little changed, we have got a good reference point. Another method requesting a reference mechanism is that by Strelitz (1980), designed to invert body waves.

Relative method developed by Dahm (1996) avoids the necessity to have a reference mechanism and, thus, seems to be highly prospective for application to groups of events which lack one distinctive individual among others, e.g., for earthquake swarms or for volcanic seismicity.

To derive the formalism by Dahm (1996), we rewrite the linear equation

$$u_n = \Sigma_{k=1,\dots,6} G_{nk}\, m_k$$

by applying the advantage of the ray approach, when six k-components of the Green function G_{nk} for the direction *n* reduce to a product of a scalar function of the particular ray and weighting terms composed of goniometric functions of the azimuth and take-off angle for the ray. Then, the equation relating ground displacement and the moment takes the form

$$u_{ij}^{n} = I_j^n \Sigma_{k=1,\dots,6}\, a_{jk}\, m_{ki}, \qquad (1)$$

where we added explicit indices *i* for event and *j* for ray. Thus, I_j^n is the above mentioned j-th ray amplitude for the n-th component of the ground motion, a_{jk} is the k-th angular function of the j-th ray (it depends also of the type of the phase just

considered, i.e. whether we are dealing with P, SV or SH), and m_{ki} is the k-th component of the moment tensor for the i-th event.

Properties of the medium affect both the terms in which the Green function was split, i.e. a_{jk} as well as I_j^n. However, a_{jk} is determined by the geometry of the ray only, whereas I_j^n is the ray amplitude, thus, it is distorted much more severely by our ignorance of the proper structural model. Therefore, it is reasonable to eliminate it by considering two events of the same location

$$u_{1j} \Sigma_{l=1,\dots,6} a_{jl} m_{l2} = u_{2j} \Sigma_{k=1,\dots,6} a_{jk} m_{k1} \qquad (2)$$

With *m* observations (i.e., *2m* phase amplitudes from 2 sources) we have

$$\begin{bmatrix} f_1 \\ f_2 \\ \vdots \\ \vdots \\ f_m \end{bmatrix} = \begin{bmatrix} u_{11}a_{11} & u_{11}a_{12} & \dots & u_{11}a_{16} \\ u_{12}a_{21} & u_{12}a_{22} & \dots & u_{12}a_{16} \\ \vdots & \vdots & & \vdots \\ \vdots & \vdots & & \vdots \\ u_{1m}a_{m1} & u_{1m}a_{21} & \dots & u_{1m}a_{m6} \end{bmatrix} \cdot \begin{bmatrix} m_{12} \\ m_{22} \\ \vdots \\ \vdots \\ m_{62} \end{bmatrix} \qquad (3)$$

where $f_j = u_{2j} \Sigma_{k=1,\dots,6} a_{jk} m_{k1}$

This system may be considered as an algorithm for inversion with a reference mechanism: if m_{k1} (k=1,...,6) are known, eq. (3) is a system for determining m_{l2}, l=1,...,6.

Dahm (1996) further extended (3) into the relative method without a reference mechanism: with 2 sources having different radiation patterns it is possible to determine their mechanisms except a constant multiplicative factor. To avoid a homogeneous equations, the additional condition is introduced

$$\Sigma_{i=1,2} \Sigma_{k=1,\dots,6} m_{ki} = \text{constant} \neq 0 \qquad (4)$$

From (3,4) the matrix formulation follows

$$\begin{bmatrix} 0 \\ 0 \\ 0 \\ \vdots \\ \vdots \\ 0 \\ c \end{bmatrix} = \begin{bmatrix} -\mathbf{A}^2 & \mathbf{A}^1 & \mathbf{0} & \mathbf{0} & \dots & \mathbf{0} \\ -\mathbf{A}^3 & \mathbf{0} & \mathbf{A}^1 & \mathbf{0} & \dots & \mathbf{0} \\ -\mathbf{A}^4 & \mathbf{0} & \mathbf{0} & \mathbf{A}^1 & \dots & \mathbf{0} \\ \vdots & \vdots & \vdots & \vdots & & \vdots \\ \vdots & \vdots & \vdots & \vdots & & \vdots \\ -\mathbf{A}^n & \mathbf{0} & \mathbf{0} & \mathbf{0} & \dots & \mathbf{A}^1 \\ \mathbf{1} & \mathbf{1} & \mathbf{1} & \mathbf{1} & \dots & \mathbf{1} \end{bmatrix} \begin{bmatrix} \mathbf{S}^1 \\ \mathbf{S}^2 \\ \mathbf{S}^3 \\ \vdots \\ \vdots \\ \mathbf{S}^n \end{bmatrix} \qquad (5)$$

with

$$\mathbf{A}^1 = \begin{bmatrix} u_{i1}a_{11} & u_{i1}a_{12} & \dots & u_{i1}a_{16} \\ u_{i2}a_{21} & u_{i2}a_{22} & \dots & u_{i2}a_{16} \\ \vdots & \vdots & & \vdots \\ \vdots & \vdots & & \vdots \\ u_{im}a_{m1} & u_{im}a_{m2} & \dots & u_{im}a_{m6} \end{bmatrix}$$

$\mathbf{1} = (1,1,1,1,1,1)$

$\mathbf{S}^k = (m_{1k}, m_{2k}, \dots, m_{6k})^T$

Equations (5) are not balanced with respect to $\mathbf{A}^1$ (it plays a dominant role since it occurs n-times there). If we do not suppose any preference, we can modify (5) to balance it :

$$
\begin{bmatrix} 0 \\ 0 \\ 0 \\ \vdots \\ 0 \\ 0 \\ \\ 0 \\ 0 \\ \vdots \\ 0 \\ 0 \\ \\ 0 \\ \vdots \\ 0 \\ 0 \\ \vdots \\ \vdots \\ c \end{bmatrix} = \begin{bmatrix} -\mathbf{A}^2 & \mathbf{A}^1 & \mathbf{0} & \mathbf{0} & \dots & \mathbf{0} & \mathbf{0} \\ -\mathbf{A}^3 & \mathbf{0} & \mathbf{A}^1 & \mathbf{0} & \dots & \mathbf{0} & \mathbf{0} \\ -\mathbf{A}^4 & \mathbf{0} & \mathbf{0} & \mathbf{A}^1 & \dots & \mathbf{0} & \mathbf{0} \\ \vdots & \vdots & \vdots & \vdots & & \vdots & \vdots \\ -\mathbf{A}^{n-1} & \mathbf{0} & \mathbf{0} & \mathbf{0} & \dots & \mathbf{A}^1 & \mathbf{0} \\ -\mathbf{A}^n & \mathbf{0} & \mathbf{0} & \mathbf{0} & \dots & \mathbf{0} & \mathbf{A}^1 \\ \\ \mathbf{0} & -\mathbf{A}^3 & \mathbf{A}^2 & \mathbf{0} & \dots & \mathbf{0} & \mathbf{0} \\ \mathbf{0} & -\mathbf{A}^4 & \mathbf{0} & \mathbf{A}^2 & \dots & \mathbf{0} & \mathbf{0} \\ \vdots & \vdots & \vdots & \vdots & & \vdots & \vdots \\ \mathbf{0} & -\mathbf{A}^{n-1} & \mathbf{0} & \mathbf{0} & \dots & \mathbf{A}^2 & \mathbf{0} \\ \mathbf{0} & -\mathbf{A}^n & \mathbf{0} & \mathbf{0} & \dots & \mathbf{0} & \mathbf{A}^2 \\ \\ \mathbf{0} & \mathbf{0} & -\mathbf{A}^4 & \mathbf{A}^3 & \dots & \mathbf{0} & \mathbf{0} \\ \vdots & \vdots & \vdots & \vdots & & \vdots & \vdots \\ \mathbf{0} & \mathbf{0} & -\mathbf{A}^{n-1} & \mathbf{0} & \dots & \mathbf{A}^3 & \mathbf{0} \\ \mathbf{0} & \mathbf{0} & -\mathbf{A}^n & \mathbf{0} & \dots & \mathbf{0} & \mathbf{A}^3 \\ \vdots & \vdots & \vdots & \vdots & & \vdots & \vdots \\ \vdots & \vdots & \vdots & \vdots & & \vdots & \vdots \\ \mathbf{1} & \mathbf{1} & \mathbf{1} & \mathbf{1} & \dots & \mathbf{1} & \end{bmatrix} \begin{bmatrix} \mathbf{S}^1 \\ \\ \mathbf{S}^2 \\ \mathbf{S}^3 \\ \vdots \\ \mathbf{S}^n \end{bmatrix}
$$

The advantage of (6) over (5) is in reducing the distortion of the inversion results due to equally distributed noise.

Dahm (1996) performed an intensive testing of his method by considering data contamination by a Gaussian noise, by observing the influence of poor station coverage and by investigating the resolvability of non-double-couple components.

Test A - synthetic amplitudes:

12 stations (Fig.D1), 8 sources: #1-4 with different mechanisms
#5-8 with similar mechanisms
#3 with 5% isotropic component

6 experiments with varying number of sources, stations and modes (see Tab.)

test #1: no noise → it returns exactly the theoretical mechanisms (Figs.D2,D3)
test #2: 10% noise, sources #1-4 (different mech.) → small bias in isotr. comp.
test #5: 10% noise, sources #5-8 (similar mech.) → larger bias in isotr. comp.
test #6: as #5 but with more stations → better performance
(⇒ relative method is more effective for a cluster of similar mechanisms if enough observations are available)
test #3: P phases only → larger error
(⇒ with only P amplitudes the resolution of the P,T axes is not excellent but, in principle, the method is working)

Test B - synthetic seismograms (simulate 4 Rhinegraben earthquakes, Figs.D4,D5)
data to invert: amplitudes of direct phases (P_g, S_g) and MOHO reflected or refracted phases (P_mP, S_mP, P_m) from 7 stations, for the distribution see Fig.D6

Isotropic component determined well, the resolution of DC is poorer (Fig.D7) → somewhat surprising in comparison to tests performed with absolute methods.

References:

Aki, K. & Richards, P., 1982. Quantitative seismology, Freeman.

Backus, G.E. & Mulcahy, M., 1976a. Moment tensors and other phenomenological descriptions of seismic sources I - Continuous displacements, *Geophys. J. R. astr. Soc.*, **46**, 341-362.

Backus, G.E. & Mulcahy, M., 1976b. Moment tensors and other phenomenological descriptions of seismic sources II - Discontinuous displacements, *Geophys. J. R. astr. Soc.*, **47**, 301-330.

Gilbert, F., 1971. The excitation of the normal modes of the Earth by earthquake sources, *Geophys. J. R. astr. Soc.*, **22**, 223-226.

Dahm, T., 1996. Relative moment tensor inversion based on ray theory: theory and synthetic tests, *Geophys. J. Int.*, **124**, 245-257.

Dziewonski, A.M., Chou, T.-A., and Woodhouse, J.H., 1981. Determination of earthquake source parameters from waveform data for studies of global and regional seismicity, *J. Geoph. Res.*, **86**, 2825-2852.

Hartzell, S.H., 1978. Earthquake aftershocks as Green's functions, *Geophys. Res. Lett.*, **5**, 1-4.

Julian, B.R., 1986. Analysing seismic-source mechanisms by linear-programming method, *Geophys. J. R. astr. Soc.*, **84**, 431-443.

Julian, B.R. & Foulger, G.R., 1996. Earthquake mechanism from linear-programming inversion of seismic-wave amplitude ratios, *Bull. seism. Soc. Am.*, **86**, 972-980.

Kisslinger, C., Bowman, J.R., & Koch, K., 1981. Procedures for computing focal mechanisms from local $(SV/P)_z$ data, *Bull. seism. Soc. Am.*, **71**, 1719-1729.

Koch, K., 1991. Moment tensor inversion of local earthquake data - I. Investigation of the method and its numerical stability with model calculations, *Geophys. J. Int.*, **106**, 305-319.

Kolář, P., 1994. Simultaneous determination of the source mechanism and the seismic wave energy, *PAGEOPH*, 143, 655-671.

Mao, W.J., Panza, G.F. & Suhadolc, P., 1994. Linearized waveform inversion of local and near-regional events for source mechanism and rupture processes, *Geophys. J. Int.*, **116**, 784-798.

Mendiguren, J., 1977. Inversion of surface wave data in source mechanism studies, *J. Geoph. Res.*, **82**, 889-894.

Patton, H., 1980. Reference point equalization for determining the source and path effects of surface waves, *J. Geoph. Res.*, **85**, 821-848.

Pearce, R.G., 1977. Fault plane solutions using relative amplitudes of P and pP, *Geophys. J. R. astr. Soc.*, **50**, 381-394.

Plicka, V., 1995. Modelling the earthquakes by empirical Green function (in Czech), *MSc Thesis*, Charles University, Prague.

Press, W.H., Teukolsky, S.A., Vetterling, W.T. & Flannery, B.P., 1992. Numerical recipes, Cambridge University Press.

Riedesel, M.A. & Jordan, T.H., 1989. Display and assessment of seismic moment tensors, *Bull. seism. Soc. Am.*, **79**, 85-100.

Ruff, L.J. & Tichelaar, B.W., 1990. Moment tensor rate functions for the 1989 Loma Prieta earthquake, *Geophys. Res. Lett.*, **17**, 1187-1190.

Ruff, L.J. & Miller, A.D., 1994. Rupture process of large earthquakes in the northern Mexico subduction zone, *PAGEOPH*, **142**, 101-172.

Šílený, J., Panza, G.F. & Campus, P., 1992. Waveform inversion for point source moment tensor retrieval with variable hypocentral depth and structural model, *Geophys. J. Int.*, **109**, 259-274.

Šílený J. & Pšenčík, I., 1995. Mechanisms of local earthquakes in 3-D inhomogeneous media determined by waveform inversion, *Geophys. J. Int.*, **121**, 459-474.

Šílený J., Campus, P. & Panza, G.F., 1996. Seismic moment tensor resolution by waveform inversion of few local noisy records - I.Synthetic tests, *Geophys. J. Int.*, **126**, 605-619.

Sipkin, S.A., 1982. Estimation of earthquake source parameters by the inversion of waveform data: synthetic waveforms, *Phys. Earth Planet. Inter.*, **30**, 242-259.

Silver, P.G. & Jordan., T.H., 1982. Optimal estimation of scalar seismic moment, *Geophys. J. R. astr. Soc.*, **70**, 755-787.

Strelitz, R.A., 1980. The fate of the downgoing slab: a study of the moment tensors from body waves of complex dee-focus earthquakes, *Phys. Earth Planet. Int.*, **21**, 83-96.

Stump, B.V. & Johnson, L.R., 1977. The determination of source properties by the linear inversion of seismograms, *Bull. seism. Soc. Am.*, 67, 1489-1502.

Takei, Y. & Kumazawa, M., 1995. Phenomenological representation and kinematics of general seismic sources including the seismic vector modes, *Geophys. J. Int.*, **121**, 641-662.

Tarantola, A., 1987. Inverse Problem Theory. Methods for data fitting and model parameter estimation, Elsevier, Amsterdam.

Tichelaar, B. & Ruff, L., 1989. How good are our best models? Jackknifing, bootstrapping and earthquake depth. *EOS* (AGU Transactions), 70(40), 593ff.

Vasco, D.W., 1989.Deriving source-time functions using principal component analysis, *Bull. seism. Soc. Am.*, **79**, 711-730.

Vasco, D.W., 1990. Moment-tensor invariants: searching for non-double-couple earthquakes, *Bull. seism. Soc. Am.*, **80**, 354-371.

Ward, S.N., 1980. A technique for the recovery of the seismic moment tensor applied to the Oaxaca, Mexico, earthquake of November 1978, *Bull. seism. Soc. Am.*, **70**, 717-734.

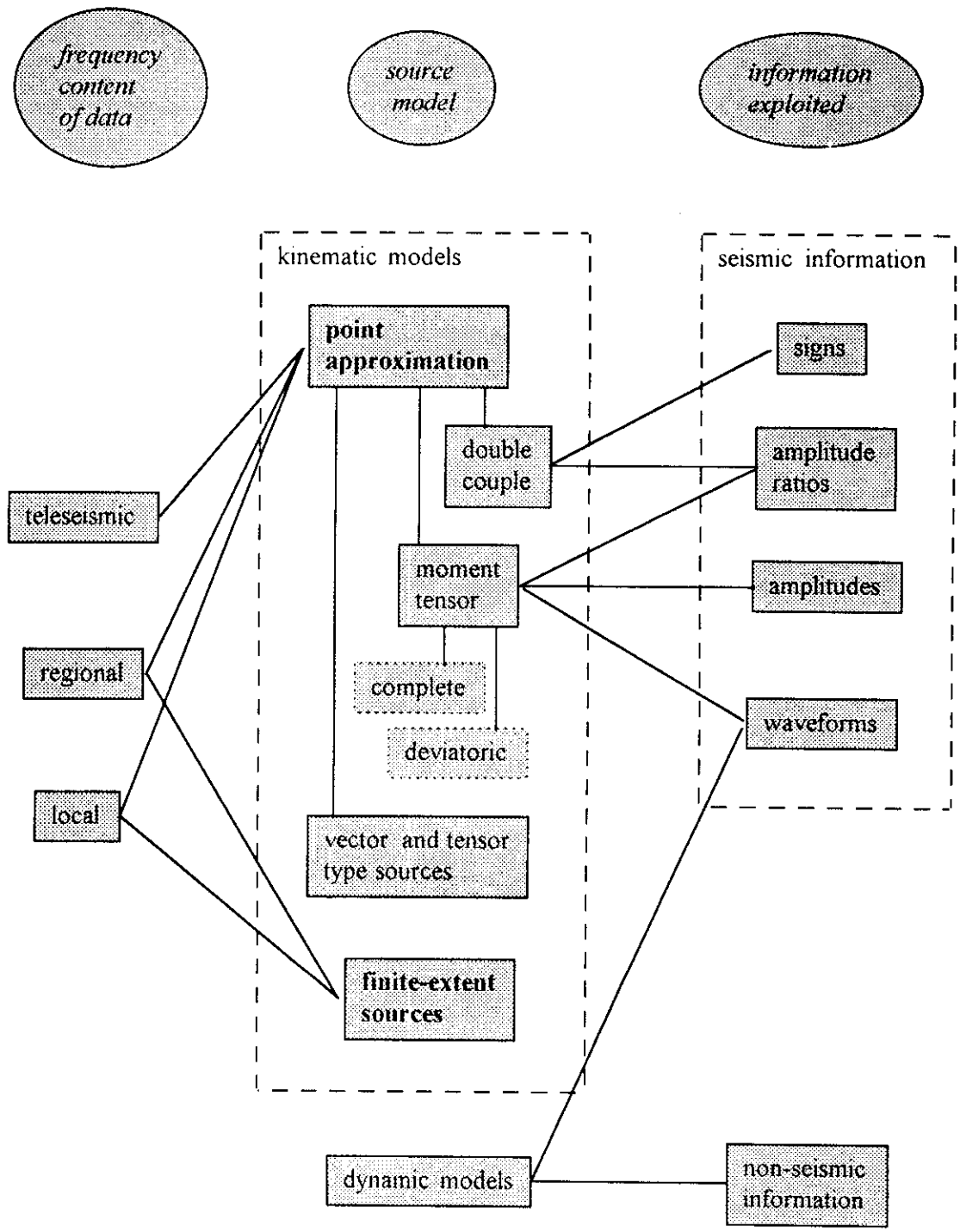
frequency content of data
source model
information exploited
kinematic models
seismic information
point approximation
double couple
moment tensor
complete
deviatoric
vector and tensor type sources
finite-extent sources
teleseismic
regional
local
signs
amplitude ratios
amplitudes
waveforms
dynamic models
non-seismic information

Fig. AR1

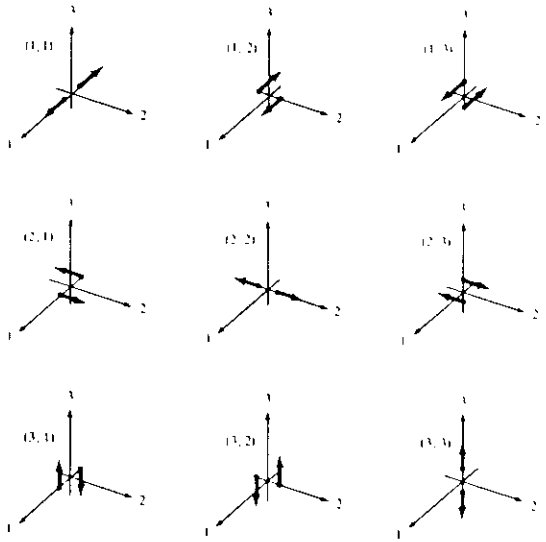

Aki, K. & Richards, P., 1982. Quantitative seismology, Freeman.

Fig. TK1

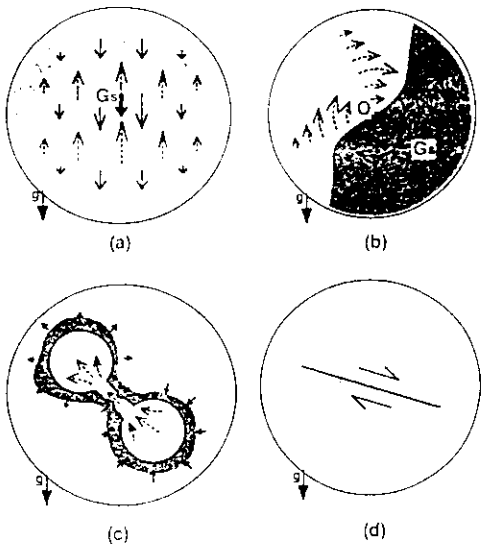

Takei, Y. & Kumazawa, M., 1995. Phenomenological representation and kinematics of general seismic sources including the seismic vector modes, *Geophys. J. Int.*, **121**, 641-662.

Fig. TK3

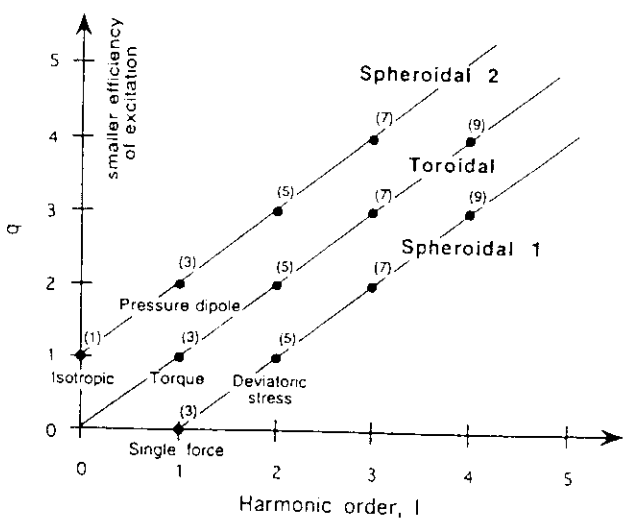

Fig. TK2

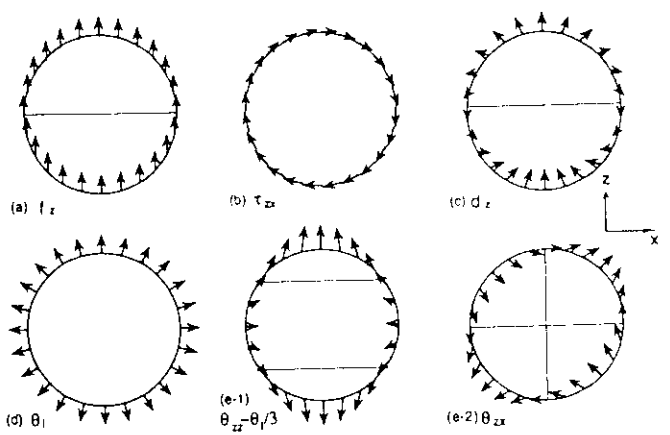

Fig. P1

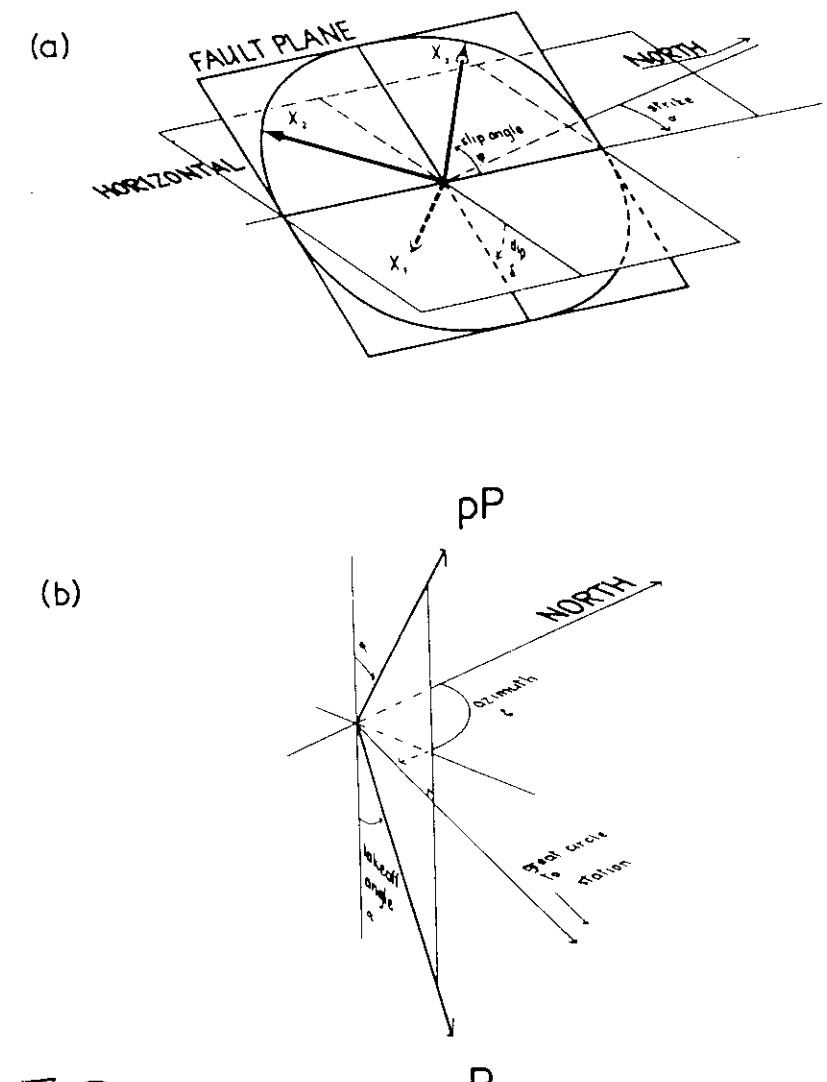

Fig. P2

Fig. P3

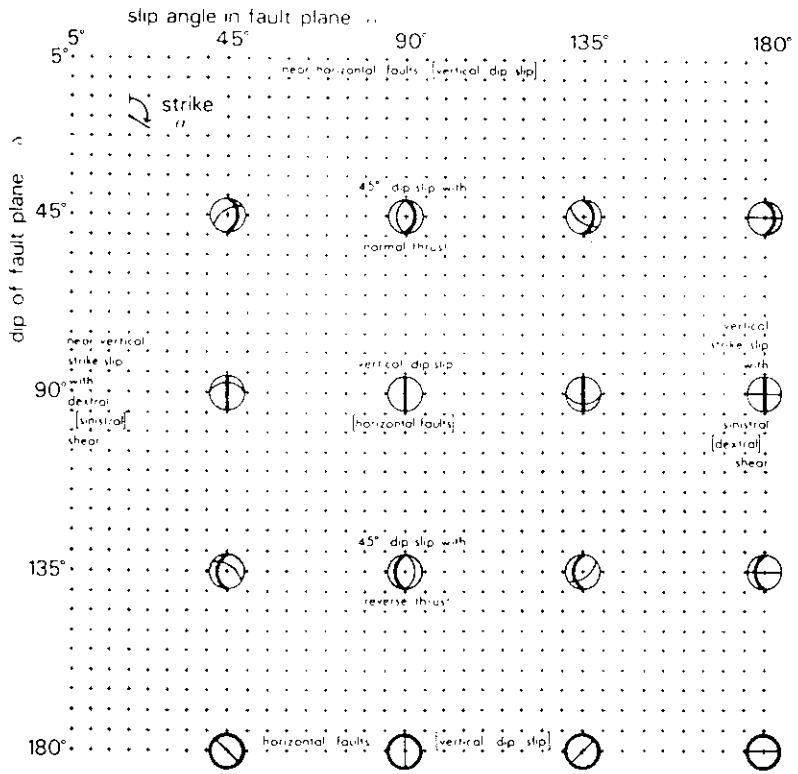

Pearce, R.G., 1977. Fault plane solutions using relative amplitudes of P and pP, *Geophys. J. R. astr. Soc.*, **50**, 381-394.

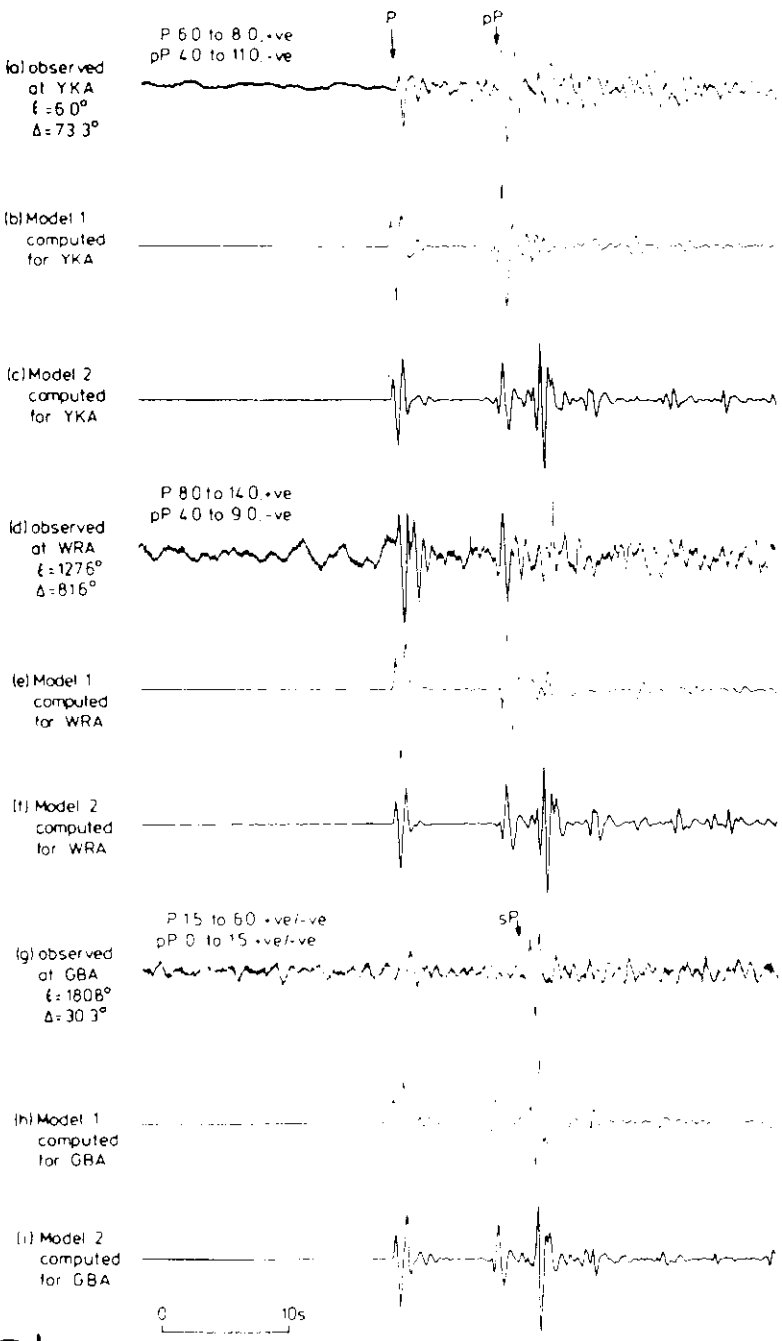

Fig. P4

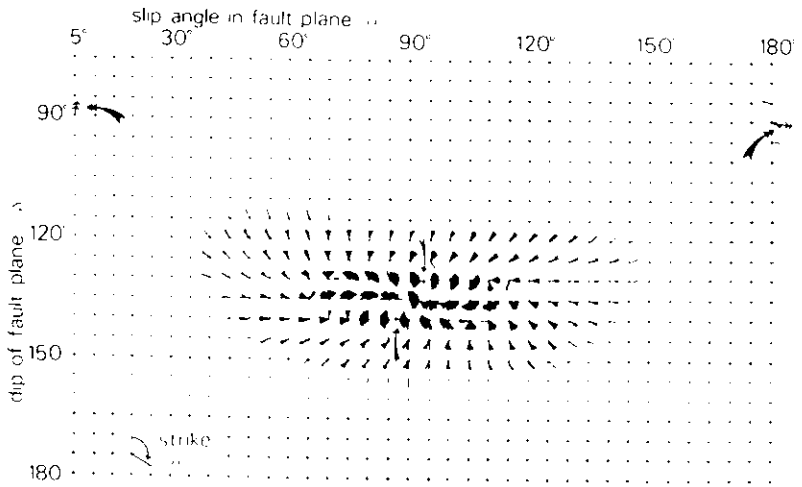

Fig. P5

Pearce, R.G., 1977. Fault plane solutions using relative amplitudes of P and pP, *Geophys. J. R. astr. Soc.*, **50**, 381-394.

Julian, B.R. & Foulger, G.R., 1996. Earthquake mechanism from linear-programming inversion of seismic-wave amplitude ratios, *Bull. seism. Soc. Am.*, **86**, 972-980.

Fig. JF1

Fig. JF3

Fig. JF2

Fig. JF4

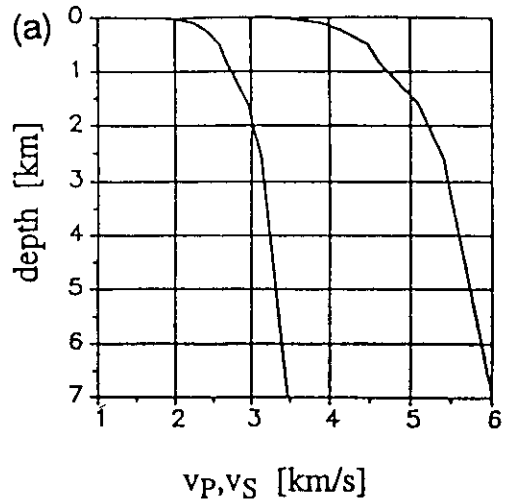

Fig. SP1

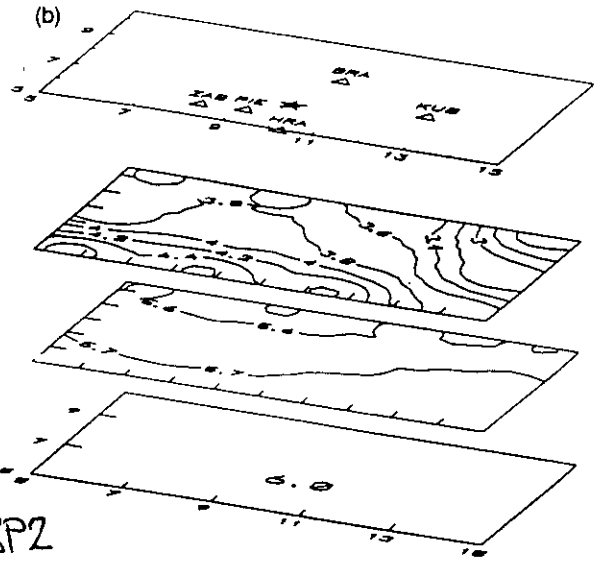

Fig. SP2

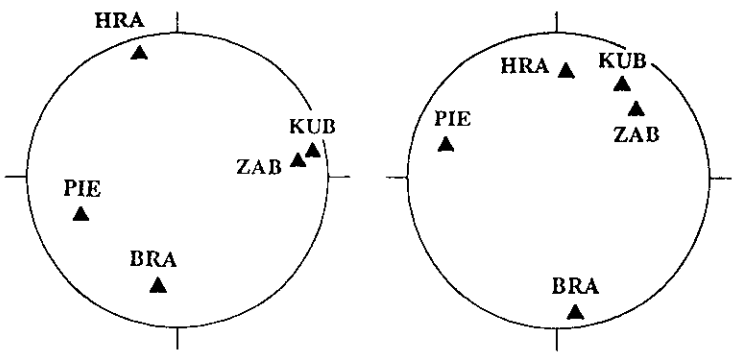

Fig. SP3

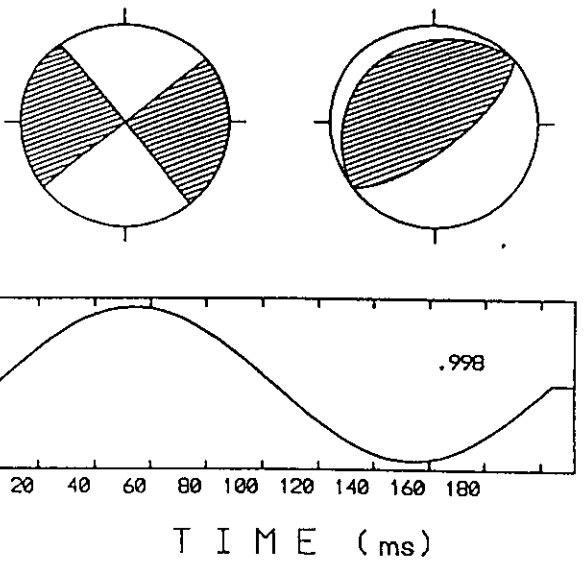

Fig. SP4

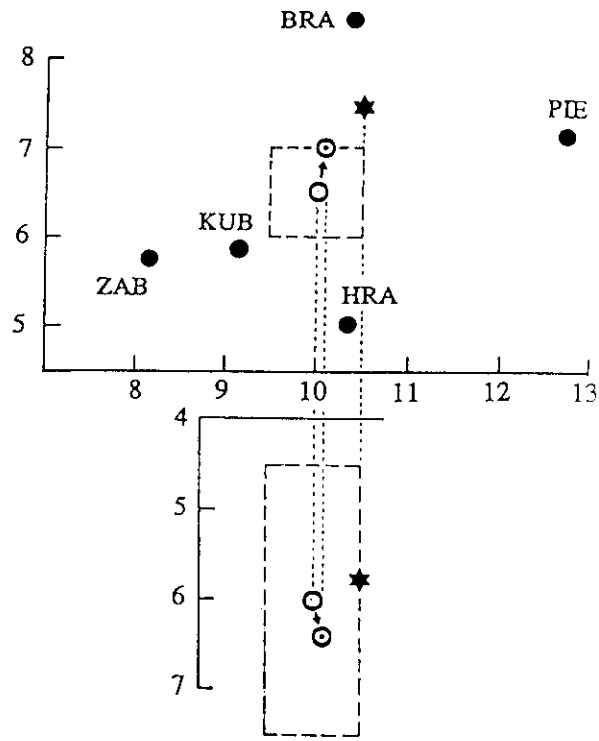

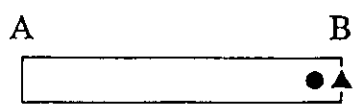

Fig. SP5

Šílený J. & Pšenčík, I., 1995. Mechanisms of local earthquakes in 3-D inhomogeneous media determined by waveform inversion, *Geophys. J. Int.*, **121**, 459-474.

Fig. SP6

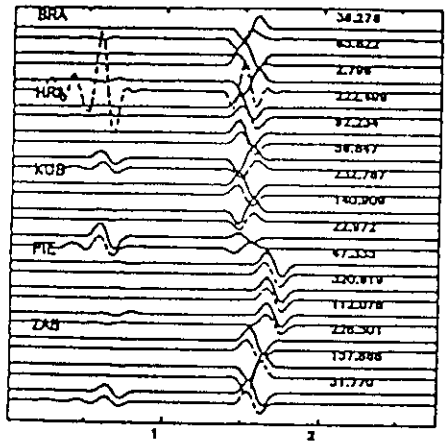

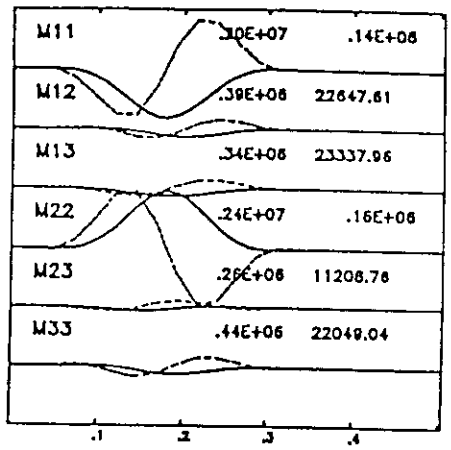

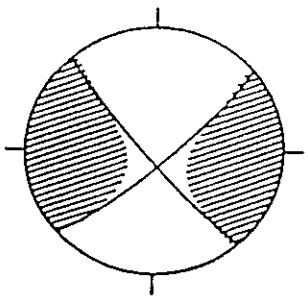

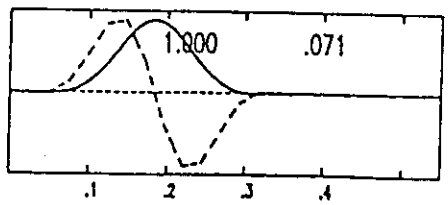

Fig. SP7

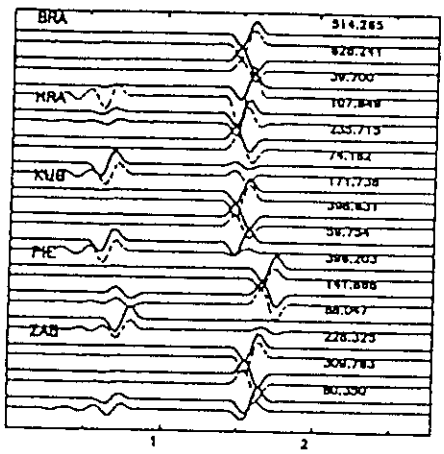

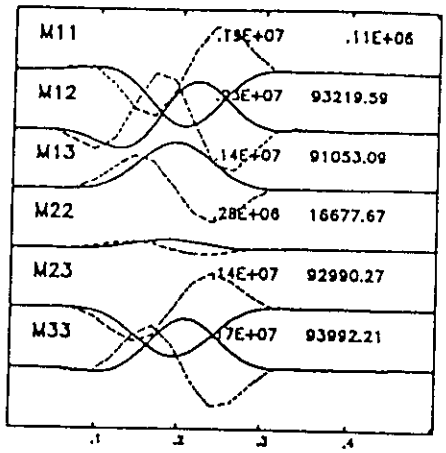

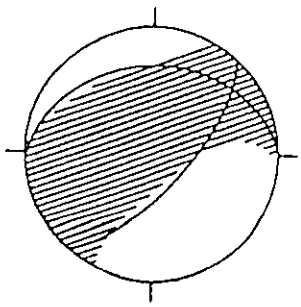

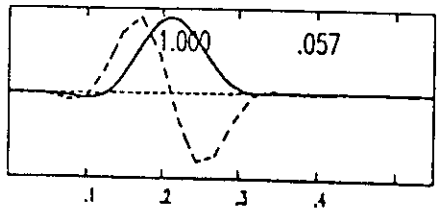

Šílený J. & Pšenčík, I., 1995. Mechanisms of local earthquakes in 3-D inhomogeneous media determined by waveform inversion. *Geophys. J. Int.*, **121**, 459-474.

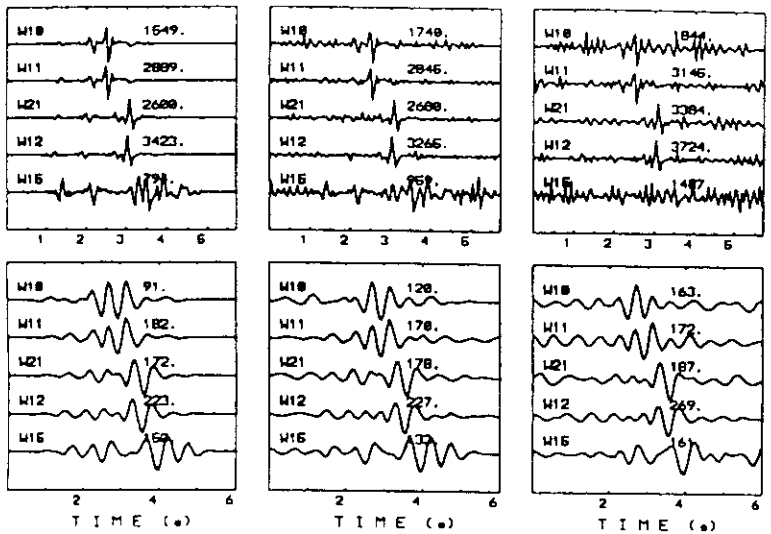

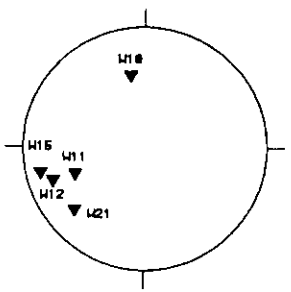

Šílený J., Campus, P. & Panza, G.F., 1996. Seismic moment tensor resolution by waveform inversion of few local noisy records - I.Synthetic tests. *Geophys. J. Int.*, **126**, 605-619.

P - waves S - waves

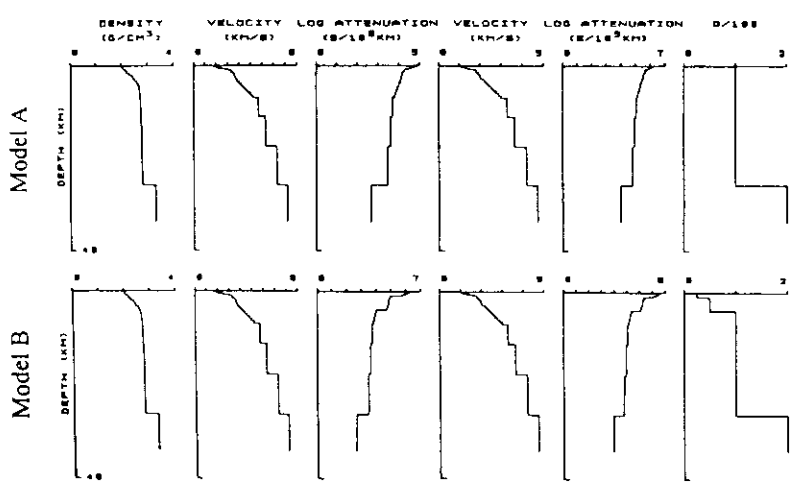

Fig. SCP1

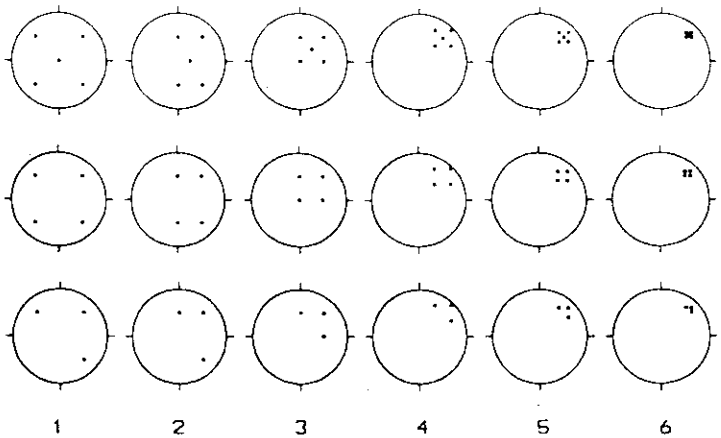

Fig. SCP2

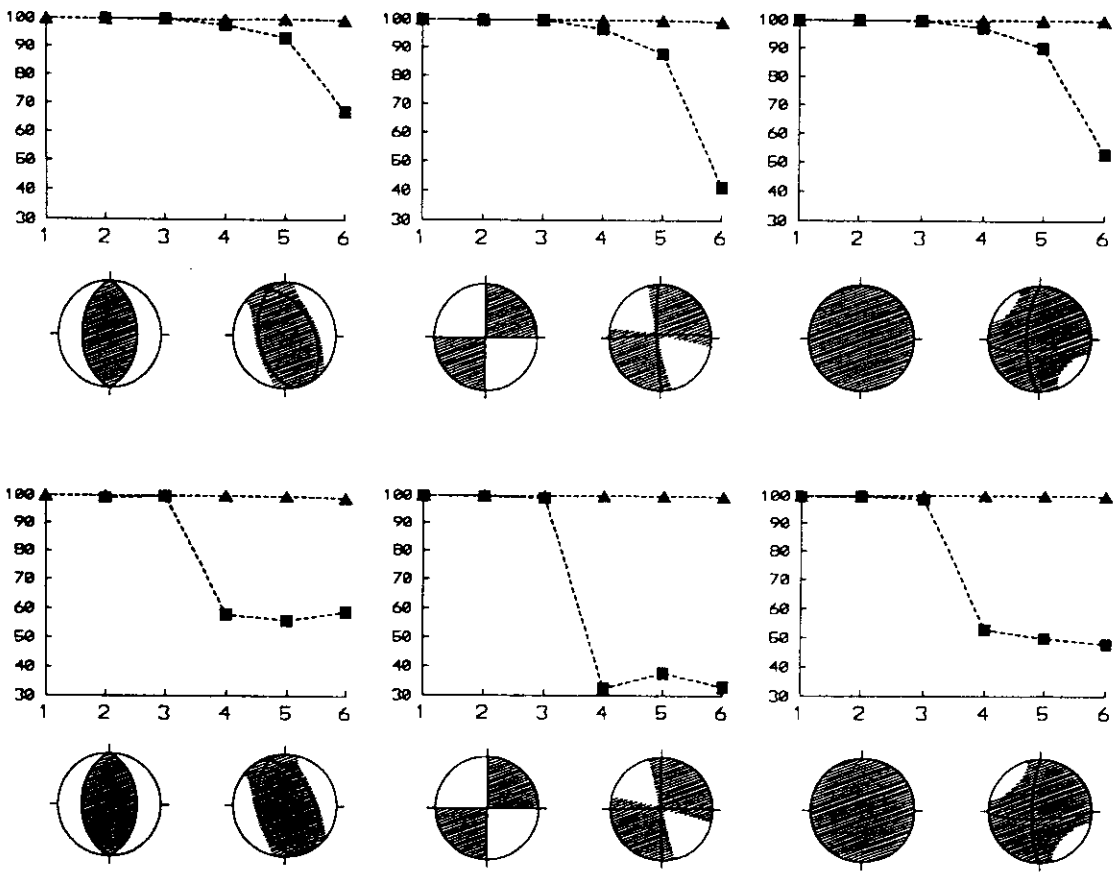

Šileny J., Campus, P. & Panza, G.F., 1996. Seismic moment tensor resolution by waveform inversion of few local noisy records - I.Synthetic tests, *Geophys. J. Int.*, **126**, 605-619

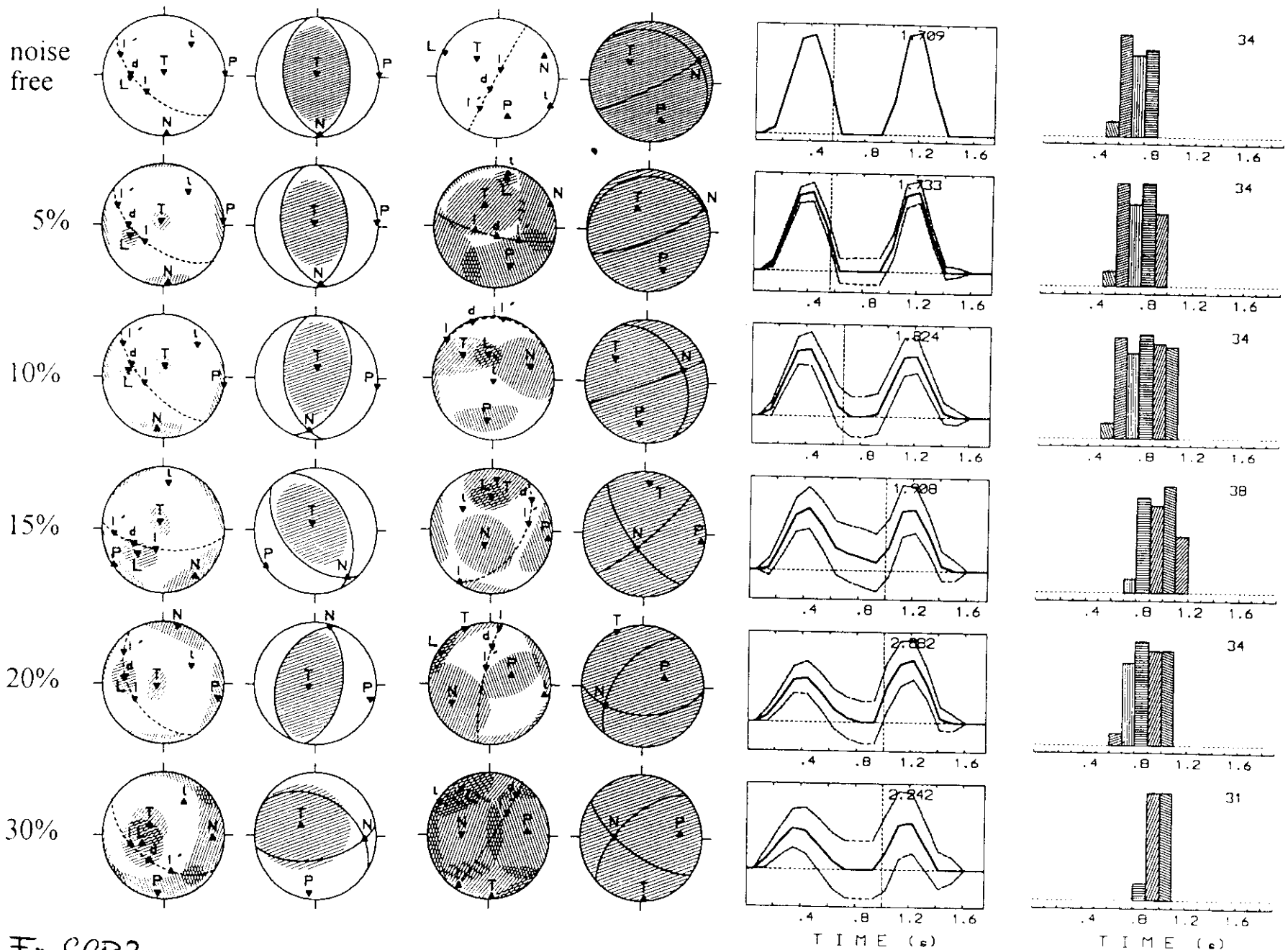

Fig. SCP3

Plicka, V., 1995: Modelling the earthquakes by empirical Green function (in Czech), *MSc Thesis*, Charles University, Prague.

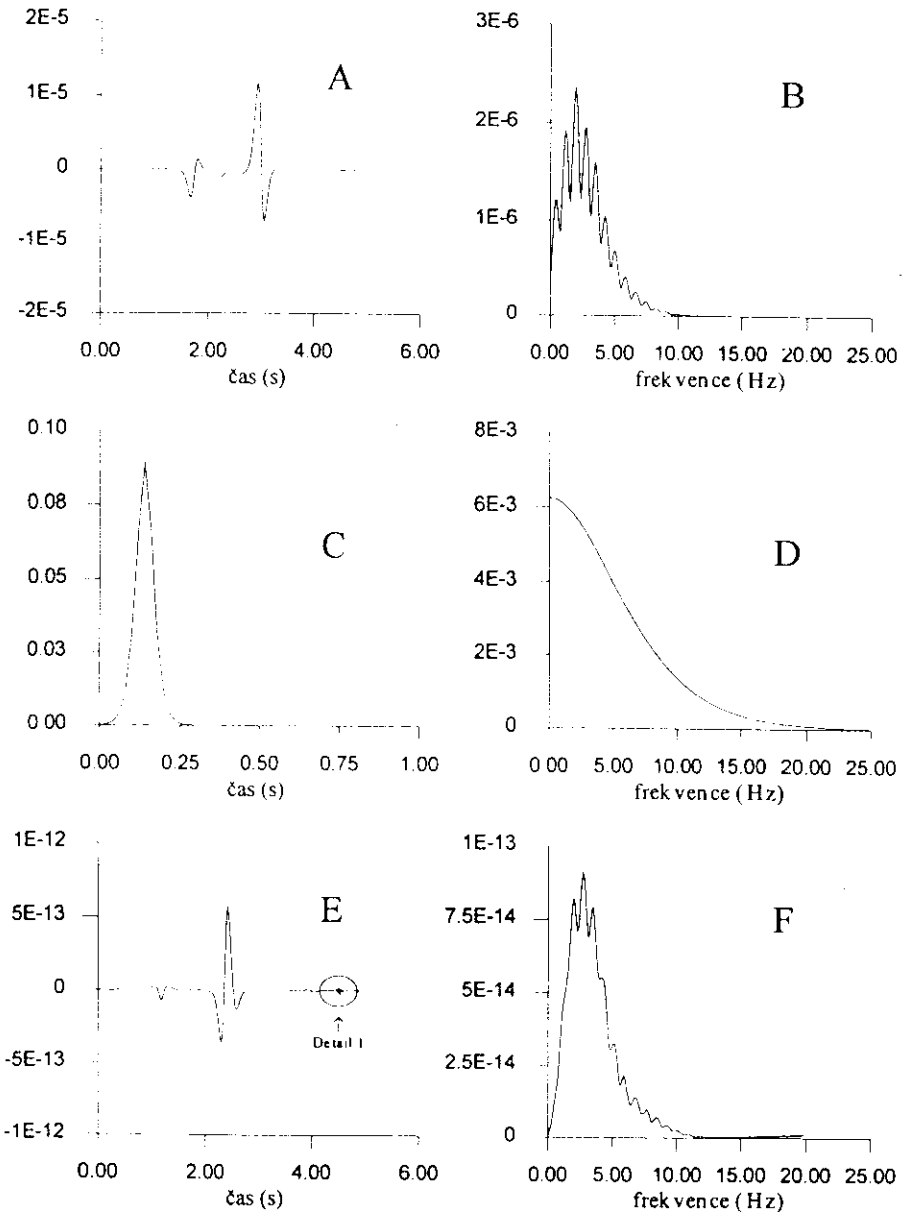

Fig. PL1

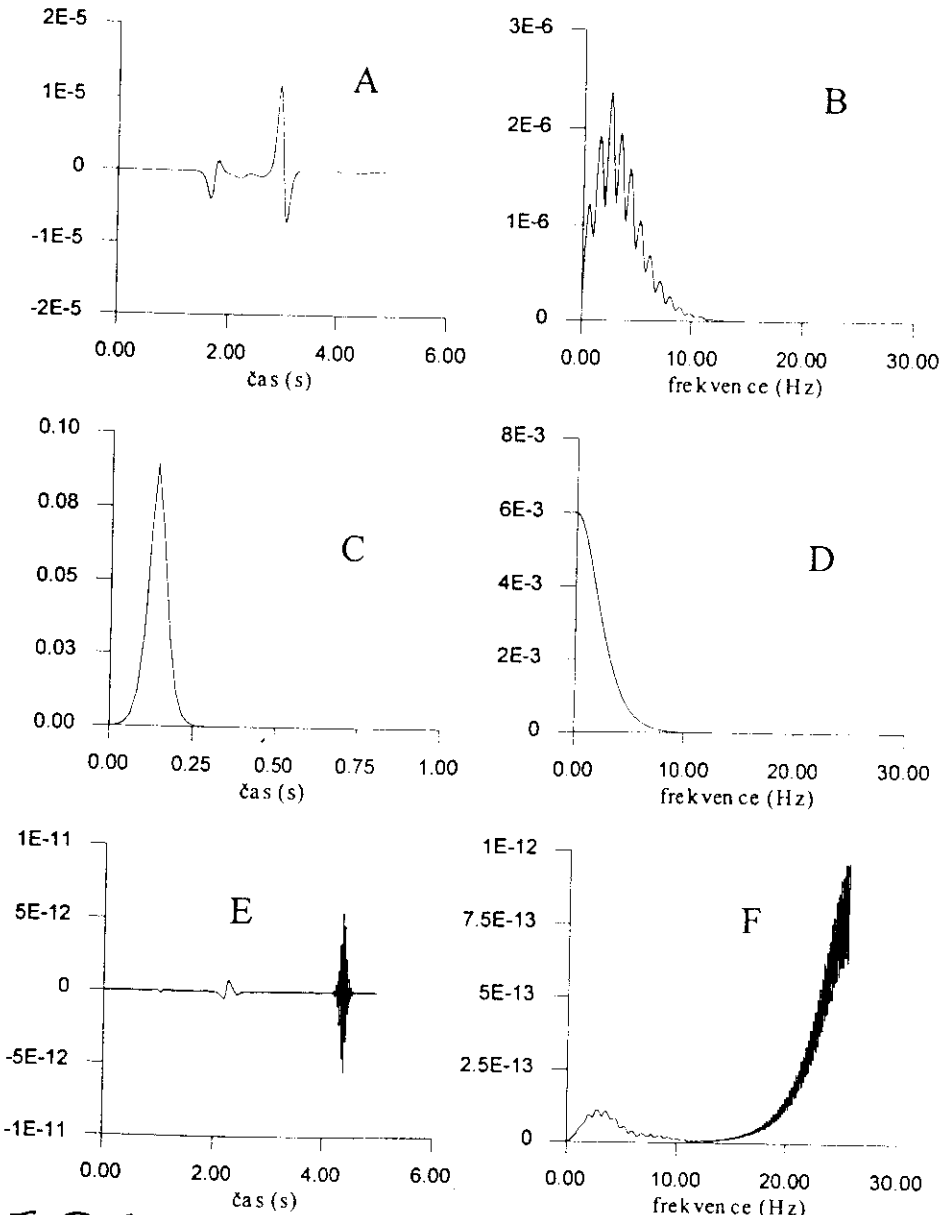

Fig. PL2

Plicka, V., 1995. Modelling the earthquakes by empirical Green function (in Czech), *MSc Thesis*, Charles University, Prague.

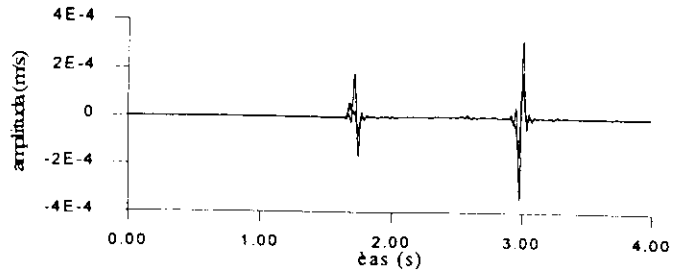

jev č .1

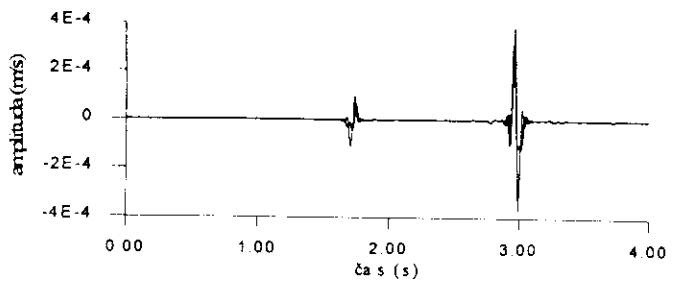

jev č .2

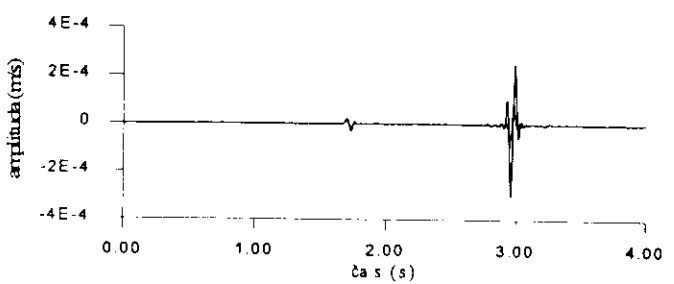

jev č .3

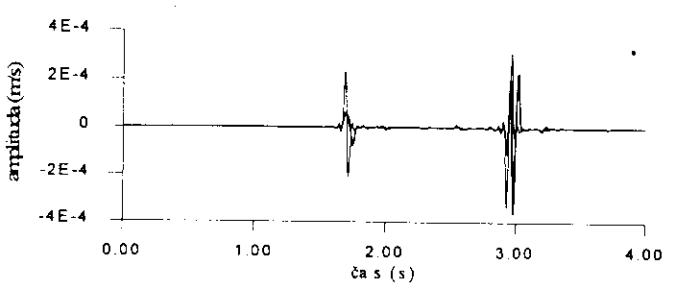

jev č.4

Fig. PL3

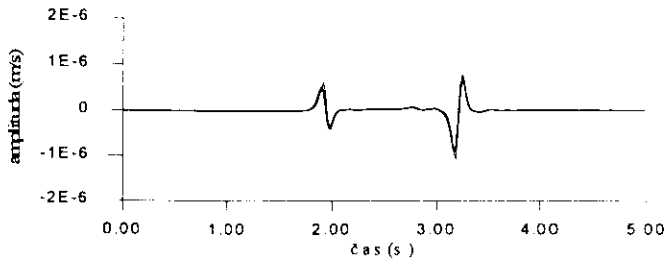

jev č. 25

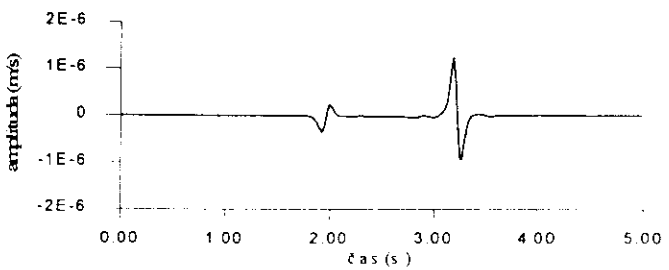

jev č. 26

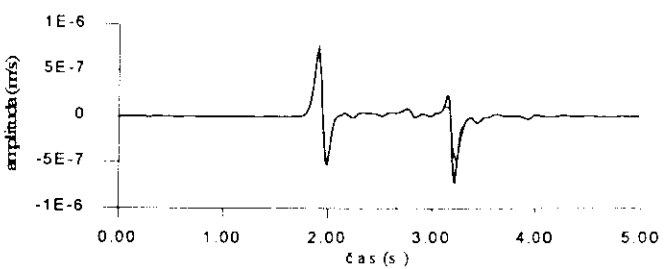

jev č. 27

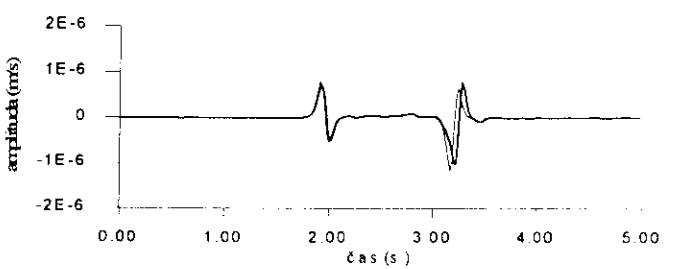

jev č. 28

Fig. PL4

Kolář, P., 1994. Simultaneous determination of the source mechanism and the seismic wave energy, *PAGEOPH*, 143, 655-671.

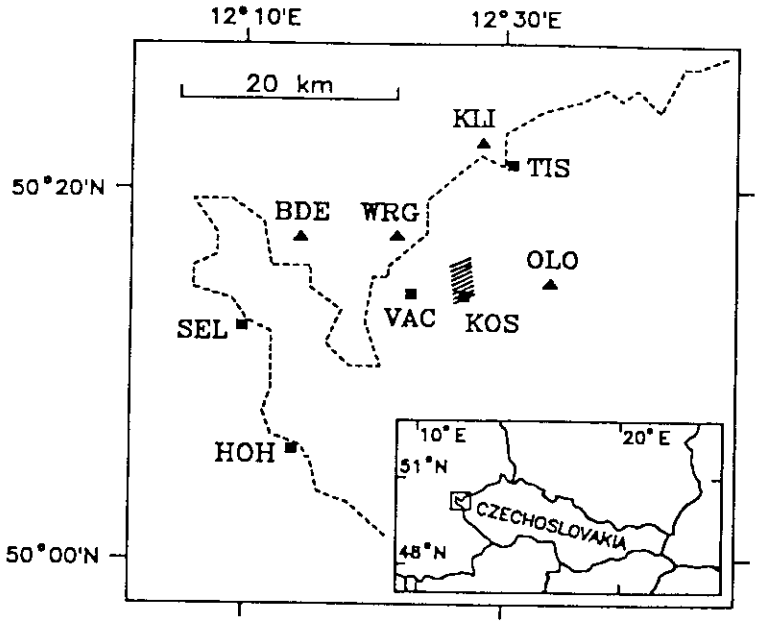

Fig. PL5

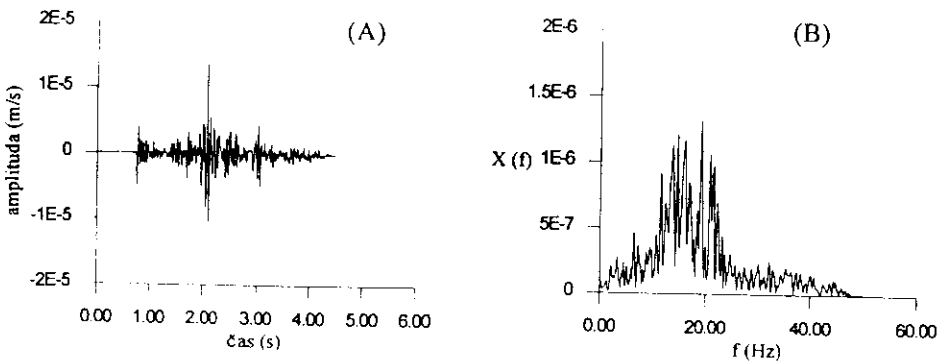

Fig. PL6

Plicka, V., 1995. Modelling the earthquakes by empirical Green function (in Czech), *MSc Thesis*, Charles University, Prague.

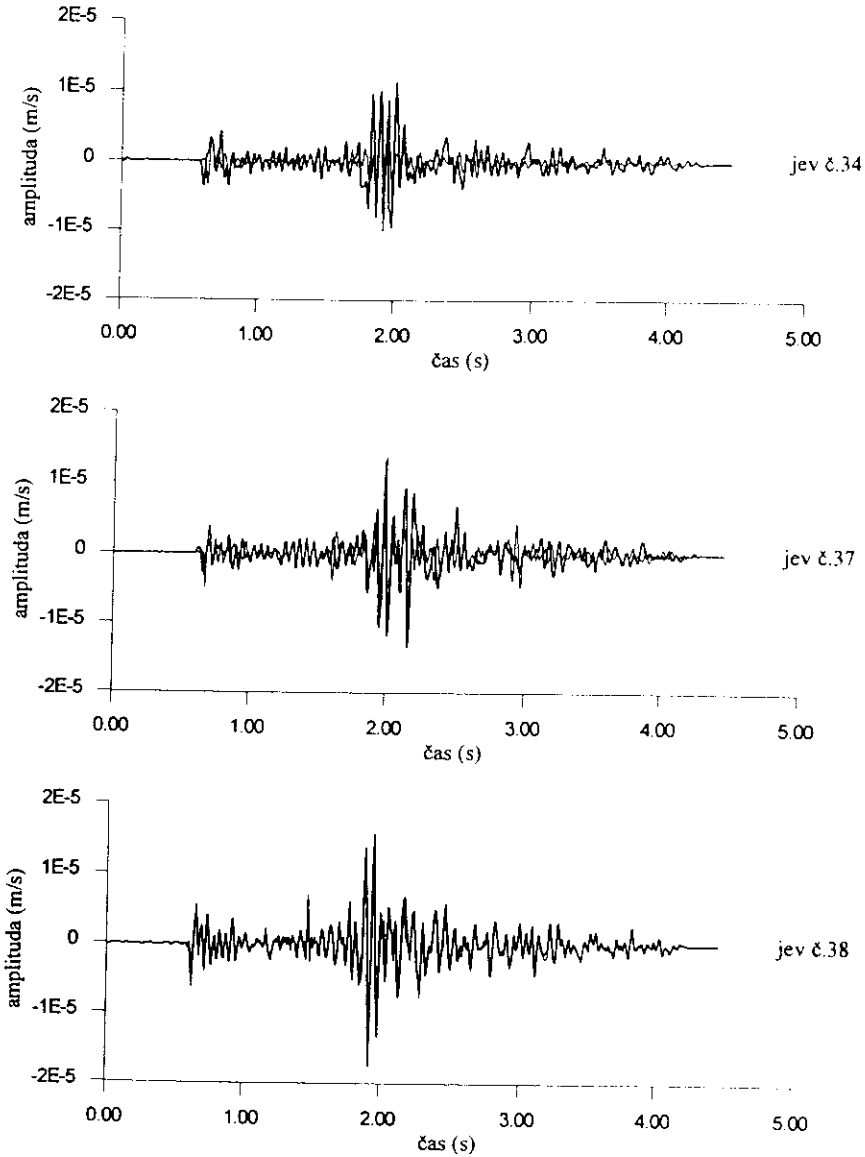

Fig. PL7

Fig. D1

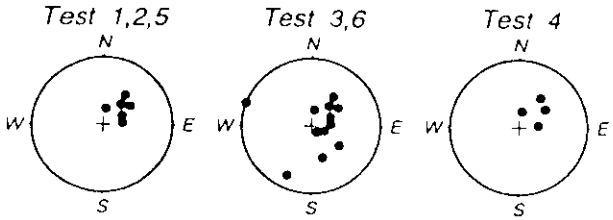

	sources	stations	wave types	noise
Test A.1	1 to 8	1 to 6	P, SH, SV	0%
Test A.2	1 to 4	1 to 6	P, SH, SV	10%
Test A.3	1 to 4	1 to 12	P	10%
Test A.4	1 to 8	1 to 4	P, SH, SV	10%
Test A.5	5 to 8	1 to 6	P, SH, SV	10%
Test A.6	5 to 8	1 to 12	P, SH, SV	10%

Dahm, T., 1996. Relative moment tensor inversion based on ray theory: theory and synthetic tests, *Geophys. J. Int.*, **124**, 245-257.

Fig. D2

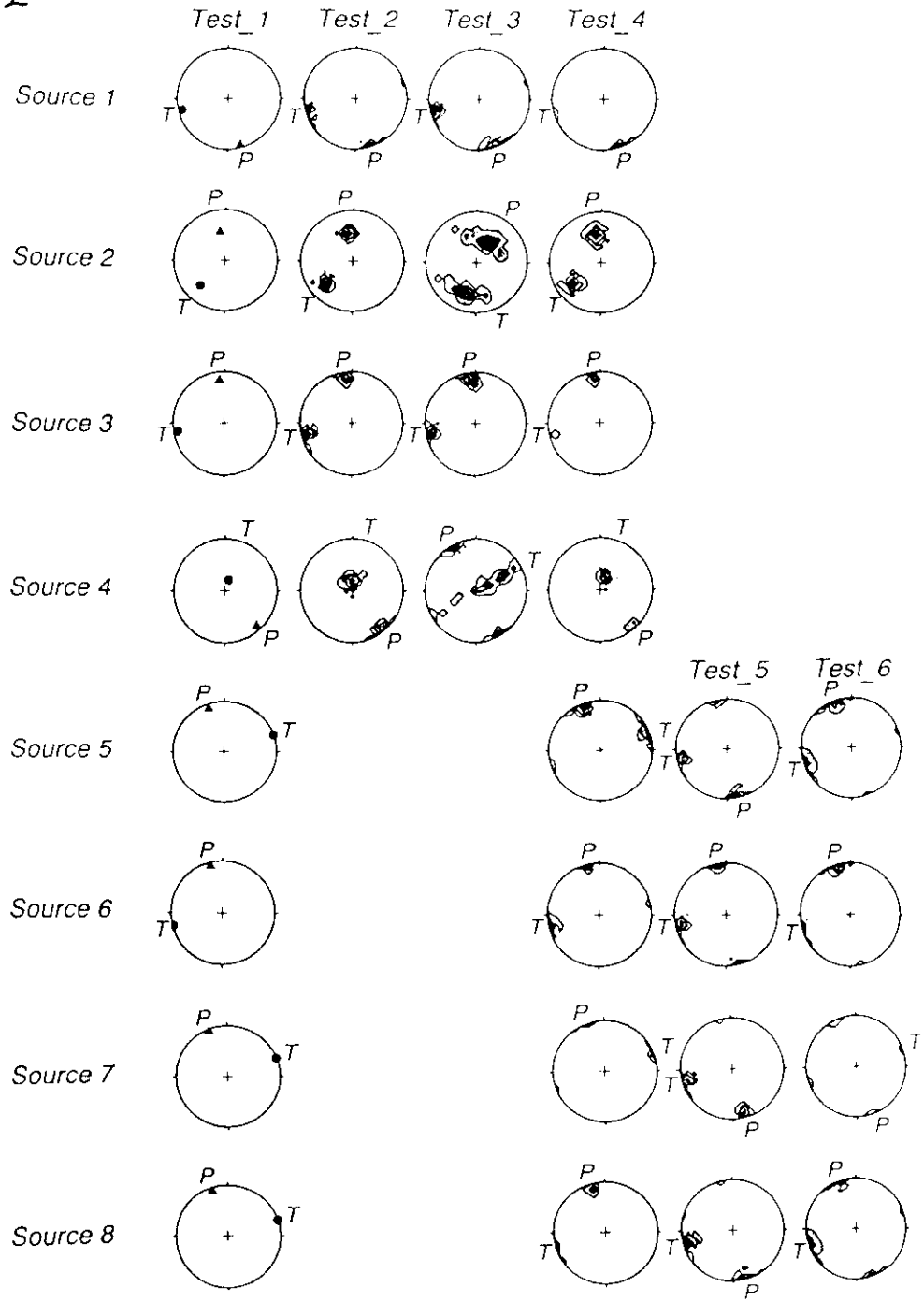

Dahm, T., 1996. Relative moment tensor inversion based on ray theory: theory and synthetic tests, *Geophys. J. Int.*, **124**, 245-257.

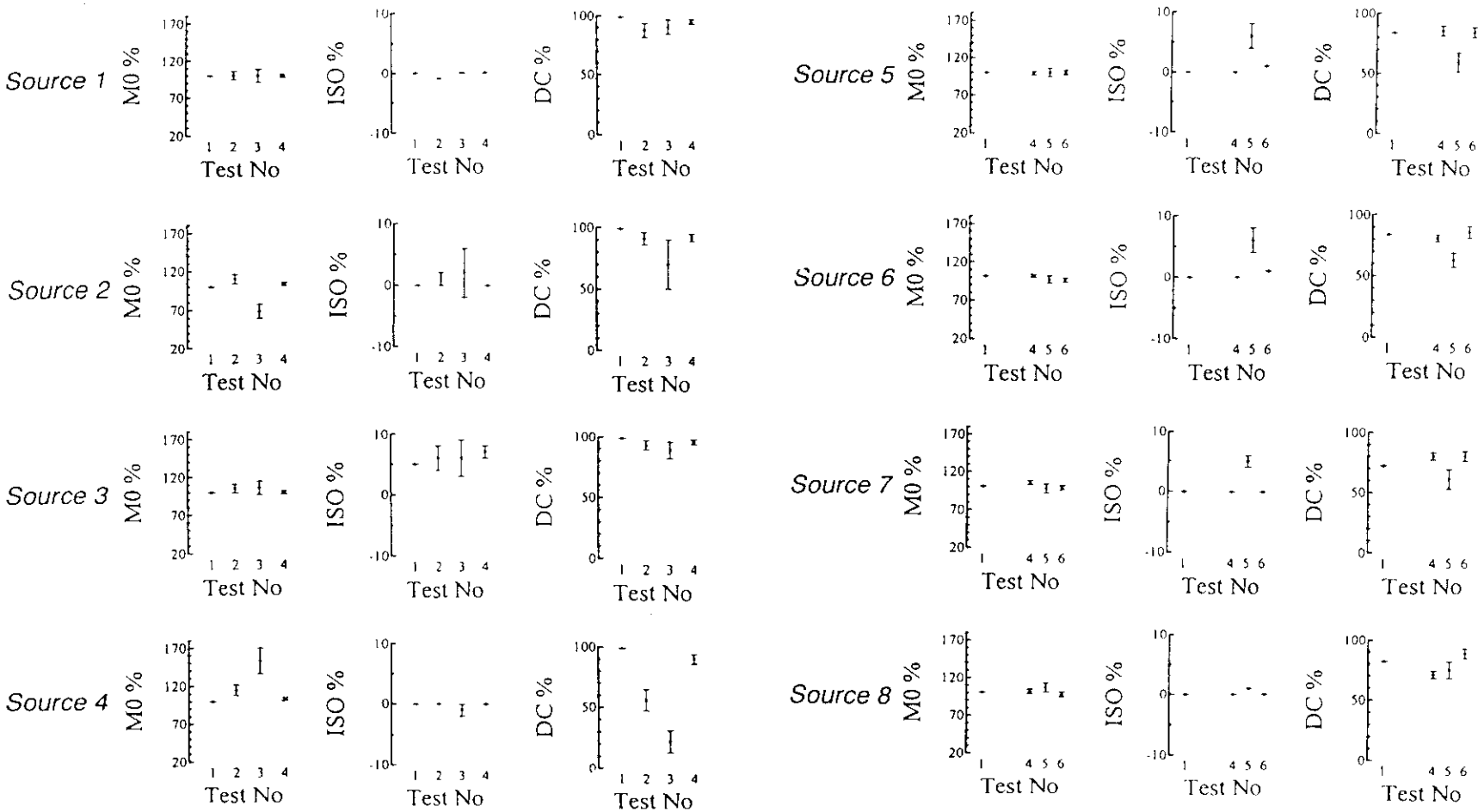

Fig. D3

Dahm, T., 1996. Relative moment tensor inversion based on ray theory: theory and synthetic tests, *Geophys. J. Int.*, **124**, 245-257.

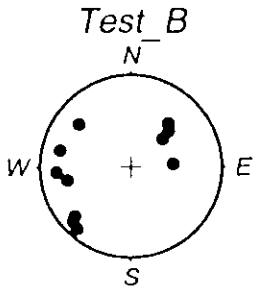

Fig. D6

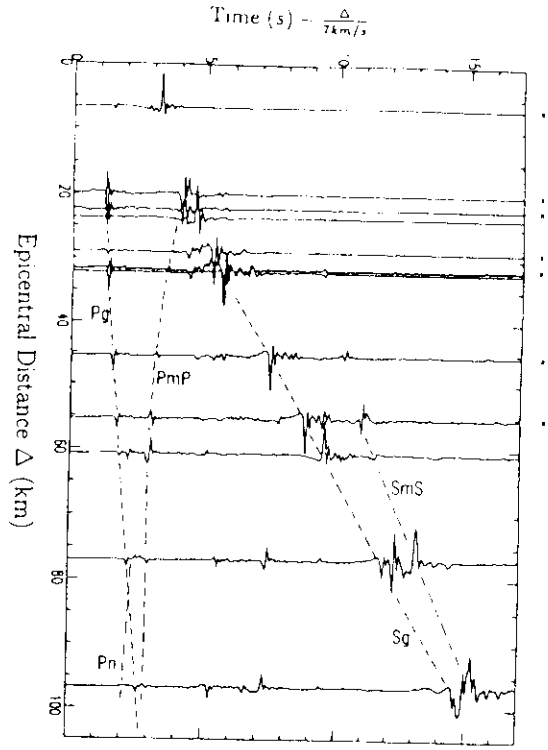

Fig. D4

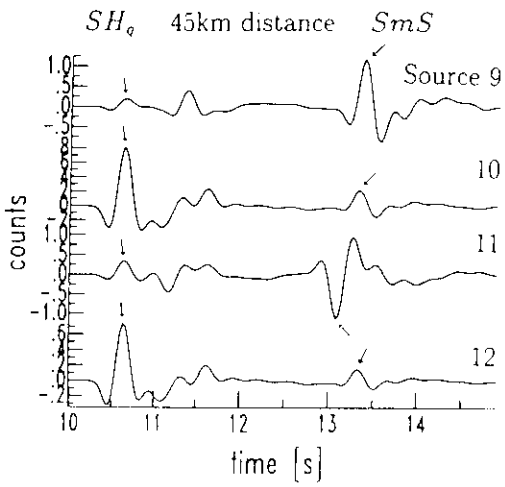

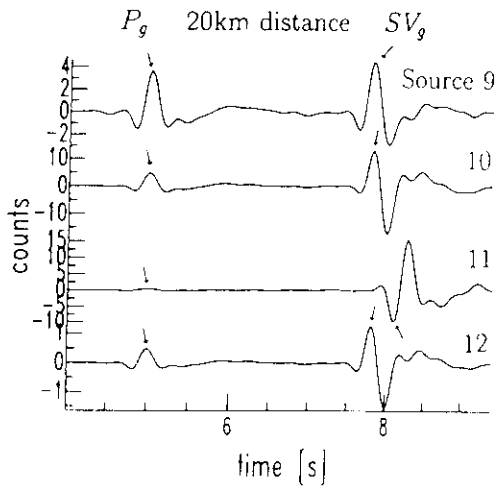

Fig. D5

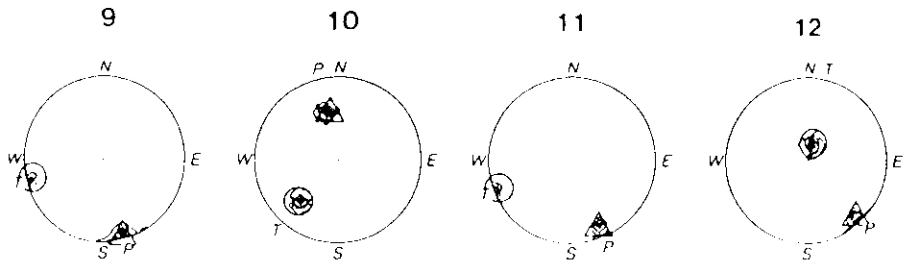

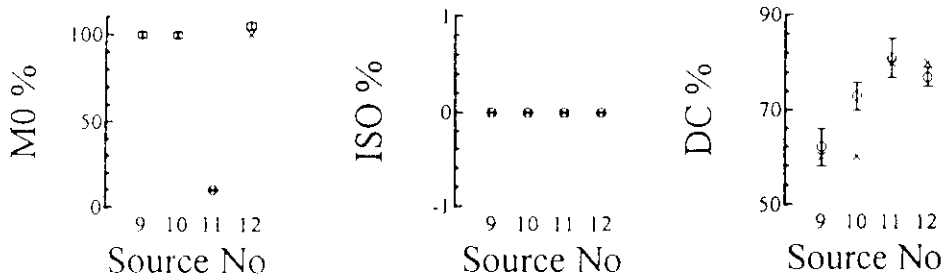

Fig. D7